# Synthesis and biological evaluation of 18F-labeled fluoropropyl tryptophan analogs as potential PET probes for tumor imaging

**ARTICLE** *in* EUROPEAN JOURNAL OF MEDICINAL CHEMISTRY · OCTOBER 2013

Impact Factor: 3.45 · DOI: 10.1016/j.ejmech.2013.10.054 · Source: PubMed

European Journal of Medicinal Chemistry 70 (2013) 768–780

Contents lists available at ScienceDirect

European Journal of Medicinal Chemistry

journal homepage: http://www.elsevier.com/locate/ejmech

Original article

# Synthesis and biological evaluation of $^{18}$F-labeled fluoropropyl tryptophan analogs as potential PET probes for tumor imaging

Aristeidis Chiotellis [a], Linjing Mu [b], Adrienne Müller [a], Svetlana V. Selivanova [a], Claudia Keller [a], Roger Schibli [a,b,c], Stefanie D. Krämer [a], Simon M. Ametamey [a,*]

[a] Center for Radiopharmaceutical Sciences ETH-PSI-USZ, Institute of Pharmaceutical Sciences ETH, Zurich, Switzerland
[b] Center for Radiopharmaceutical Sciences ETH-PSI-USZ, Department of Nuclear Medicine, University Hospital Zurich, Zurich, Switzerland
[c] Center for Radiopharmaceutical Sciences ETH-PSI-USZ, Paul Scherrer Institute, Villigen, Switzerland

ARTICLE INFO

*Article history:*
Received 29 August 2013
Received in revised form
17 October 2013
Accepted 21 October 2013
Available online 30 October 2013

*Keywords:*
Amino acids
Tryptophan
Tumor imaging
PET
LAT

ABSTRACT

In the search for an efficient, fluorine-18 labeled amino acid based radiotracer for tumor imaging with positron emission tomography (PET), two new tryptophan analogs were synthesized and characterized *in vitro* and *in vivo*. Both are tryptophan alkyl-derivatives, namely 2-(3-[$^{18}$F]fluoropropyl)-DL-tryptophan ([$^{18}$F]2-FPTRP) and 5-(3-[$^{18}$F]fluoro-propyl)-DL-tryptophan ([$^{18}$F]5-FPTRP). Standard reference compounds and precursors were prepared by multi step approaches. Radiosynthesis was achieved by no-carrier-added nucleophilic [$^{18}$F]fluorination in 29–34% decay corrected yields with radiochemical purity over 99%. *In vitro* cell uptake assays showed that both compounds are substrates for amino acid transport and enter small cell lung cancer cells (NCI-H69) most probably almost exclusively via large neutral amino acids transporter(s) (LAT). Small animal PET imaging with xenograft bearing mice revealed high tumor/background ratios for [$^{18}$F]2-FPTRP comparable to the well established tyrosine analog *O*-(2-[$^{18}$F]fluroethyl)-L-tyrosine ([$^{18}$F]FET). Radiometabolite studies showed no evidence of involvement of a biotransformation step in tumor accumulation.



## 1. Introduction

The development of radiotracers with applications in oncology is a major focus of radiopharmaceutical research. Numerous studies have demonstrated that malignant tumors can be detected with high sensitivity and specificity by imaging their increased metabolic rates for glucose, amino acids, lipids and nucleosides [1,2]. PET imaging with the glucose analog [$^{18}$F]fluorodeoxyglucose ([$^{18}$F]FDG) has become a routine clinical test for staging, treatment planning and monitoring response to therapy for a number of types of cancer [3,4]. While [$^{18}$F]FDG has proven to be a very efficient imaging agent, it has certain limitations such as high physiological uptake in certain organs (brain, kidneys, urinary tract), accumulation in inflammatory tissues and low or variable uptake in certain types of malignant lesions, e.g. renal cell carcinoma and endocrine tumors [5,6].

Apart from being the building blocks of proteins, amino acids serve many other vital functions in cells. Most malignant lesions show an increased demand for amino acids due to their increased metabolic needs which is expressed via enhanced amino acid transport compared to normal cells [7–9]. In particular, the level of the heterodimer obligatory exchange transport system for large neutral amino acids, LAT1/4F2hc (LAT1) is increased in many types of human tumors and levels may correlate with the malignancy of the lesion [10–12]. In this respect, [$^{18}$F] and [$^{11}$C]-labeled amino acids are good candidates for tumor imaging by PET and unlike [$^{18}$F]FDG, they do not generally accumulate in healthy brain or inflamed tissue. A number of radiolabeled amino acids (Fig. 1) including *O*-(2-[$^{18}$F]fluroethyl)-L-tyrosine ([$^{18}$F]FET) [13,14], 3-[$^{123}$I]iodo-alpha-methyl-L-tyrosine ([$^{123}$I]IMT) [15], L-[$^{11}$C-methyl]me-

*Abbreviations:* aadc, aromatic amino acid decarboxylase; APUD, amine precursor uptake and decarboxylation; BCH, 2-amino-2-norbornanecarboxylic acid; $BF_3{\cdot}Et_2O$, boron trifluoride etherate; [$^{11}$C]5HTP, 5-hydroxy-L-[β-$^{11}$C]tryptophan; [$^{11}$C]MET, L-[$^{11}$C-methyl]methionine); EBSS, Earle balanced salt solution; [$^{18}$F]2-FPTRP, 2-(3-[$^{18}$F]fluoropropyl)-DL-tryptophan); [$^{18}$F]5-FPTRP, 5-(3-[$^{18}$F]fluoropropyl)-DL-tryptophan; [$^{18}$F]FACBC, *anti*-1-amino-3-[$^{18}$F]-fluoro-cyclobutane-1-carboxylic acid; [$^{18}$F]FDG, 2-deoxy-2-($^{18}$F)fluoro-D-glucose; [$^{18}$F]FDOPA, L-3,4-dihydroxy-6-[$^{18}$F]fluorophenylalanine; [$^{18}$F]FET, *O*-(2-[$^{18}$F]fluroethyl)-L-tyrosine; [$^{18}$F]L-FEHTP, 5-(2-[$^{18}$F]fluoroethoxy)-L-tryptophan; [$^{123}$I]IMT, 3-[$^{123}$I]iodo-alpha-methyl-L-tyrosine); LAT, large amino acid transporter; PET, positron emission tomography; SUV, standardized uptake values; $TBAHCO_3$, tetrabutylammonium bicarbonate; TBAOH, tetrabutylammonium hydroxide; TEBAC, triethylbenzylammonium chloride.

* Corresponding author. Center for Radiopharmaceutical Sciences ETH-PSI-USZ, Institute of Pharmaceutical Sciences ETH, Zurich, DCHAB, HCI H427, Wolfgang Pauli Strasse 10, 8093 Zurich, Switzerland. Tel.: +41 44 6337463.
*E-mail address:* simon.ametamey@pharma.ethz.ch (S.M. Ametamey).

0223-5234/$ – see front matter © 2013 Elsevier Masson SAS. All rights reserved.
http://dx.doi.org/10.1016/j.ejmech.2013.10.054

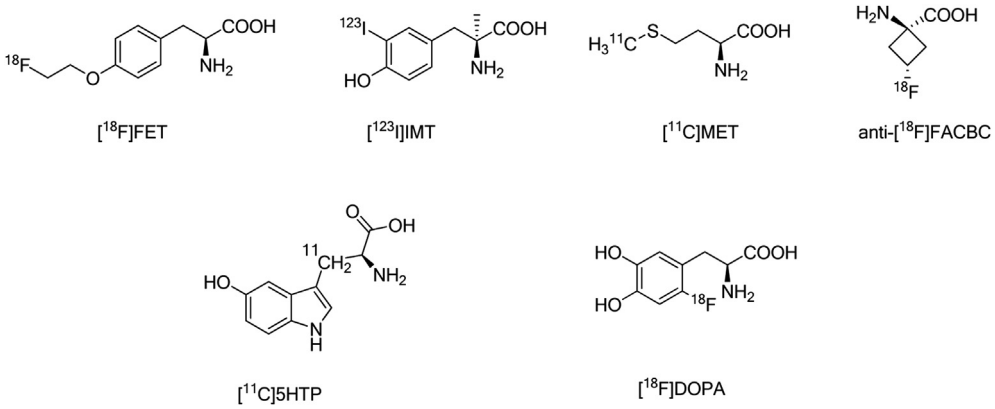


**Fig. 1.** Some clinically utilized amino acid based tracers.

thionine ([$^{11}$C]MET) [16] and *anti*-1-amino-3-[$^{18}$F]-fluorocyclobutane-1-carboxylic acid ([$^{18}$F]FACBC) [17] have proven to be useful tumor imaging agents while accumulation occurs primarily through LAT transport. The well-established dopa and tryptophan analogs L-3,4-dihydroxy-6-[$^{18}$F]fluorophenylalanine ([$^{18}$F]FDOPA) and 5-hydroxy-L-[β-$^{11}$C]tryptophan ([$^{11}$C]5HTP) respectively (Fig. 1), accumulate in endocrine tumors not only through LAT transport but also via decarboxylation by aromatic amino acid decarboxylase (AADC) [18] the level of which is enhanced in these lesions [19]. Decarboxylation of these amino acids converts them to biogenic amines which can be stored in secretory granulae, a mechanism which leads to their trapping inside the cancer cell (APUD concept, Amine Precursor Uptake and Decarboxylation) [18,20–22].

Although clinically applied with success, [$^{11}$C]5HTP has significant drawbacks. The tracer synthesis is quite complex since it relies on two multi-enzyme steps [23]. Also, the short physical half life of 20 min for $^{11}$C limits its application to facilities with on-site cyclotron. This has fueled efforts towards the development of a fluorine-18 based tryptophan tracer and to date, two new compounds have emerged; 5-(2-[$^{18}$F]fluoroethoxy)-L-tryptophan ([$^{18}$F]L-FEHTP) (Fig. 2) developed independently by Krämer et al. [24] and by Li et al. [25] and 1-[$^{18}$F]fluoroethyl-L-tryptophan reported by Sun et al. [26]. While there is still no biological evaluation for the latter tracer, 5-(2-[$^{18}$F]fluoroethoxy)-L-tryptophan was characterized pharmacologically. [$^{18}$F]L-FEHTP accumulates in endocrine and nonendocrine tumor models via LAT transport but is not decarboxylated by AADC [24].

The promising results of [$^{18}$F]L-FEHTP encouraged us to investigate structures similarly related to this compound aiming to develop a tryptophan tracer with improved *in vivo* pharmacokinetics resulting in higher tumor uptake. We chose to develop two fluoropropyl derivatives – structural analogs of [$^{18}$F]L-FEHTP where the fluoropropyl side chain is attached to either position 2- or 5- of the indole ring. The 5-position was selected so as to directly compare the new analog with the previously reported [$^{18}$F]L-FEHTP while 2-position was chosen as an innovative position for derivatization of the tryptophan core. Substitution of oxygen with carbon to construct a direct linkage of the [$^{18}$F] bearing side chain to the indole ring is expected to alter the chemical and physical characteristics of the molecule, leading to increased lipophilicity and modified electronic properties of the indole ring. Additionally, the different kind of bonding and probably most importantly, the localization of the fluoropropyl chain on the pyrrole part of the indole ring (in the case of the 2-fluoropropyl derivative), might be a way to change the *in vivo* behavior of the molecule towards being a better substrate for LAT or even being recognized by AADC. AADC exhibits broad substrate specificity [27]. Because tryptophan and 5HTP are substrates for AADC their structural modification could potentially lead to derivatives that are recognized by this enzyme. The combination of LAT1 and AADC recognition would be advantageous for endocrine tumor targeting.

In this work, we describe the synthesis, radiolabeling and biological evaluation of two new tryptophan derivatives, 2-(3-[$^{18}$F]fluoropropyl)-DL-tryptophan ([$^{18}$F]2-FPTRP) and 5-(3-[$^{18}$F]fluoropropyl)-DL-tryptophan ([$^{18}$F]5-FPTRP) (Fig. 2) and their comparison with [$^{18}$F]FET. For the *in vitro* and *in vivo* evaluations, we chose the endocrine small cell lung cancer cell line NCI-H69 and the pseudoendocrine prostate cancer cell line PC-3. The NCI-H69 cell line displays high AADC activity [28] while the PC-3 cell line has been shown to express AADC at the messenger RNA level [29]. LAT1 levels are increased in both cell lines [30,31].

## 2. Results and discussion

### 2.1. Chemistry

For the synthesis of the cold analogs and precursors, *tert*-butyl based protecting groups (Boc/*tert*-butyl ester) were employed for the protection of the functional groups of the amino acids mainly

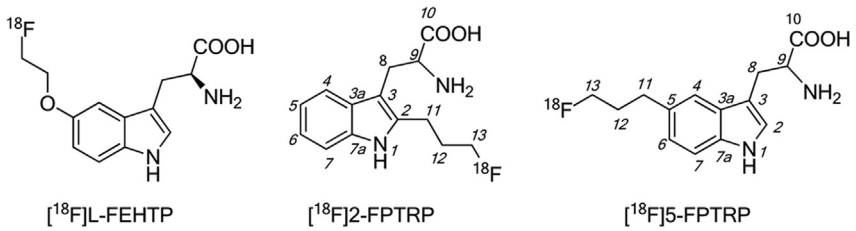


**Fig. 2.** Chemical structures of [$^{18}$F]L-FEHTP and of the new tryptophan derivatives. The numbering of the atoms of the tryptophan core and side chain is denoted for $^{1}$H and $^{13}$C NMR chemical shift assignments.

due to their robustness and stability during the synthetic sequences but also in order to simplify the radiosynthetic process in respect of achieving full deprotection in one step.

2-FPTRP was synthesized starting from commercially available DL-tryptophan as depicted in Scheme 1. We used racemic DL tryptophan as we initially wanted to verify whether the new analogs would show any notable biological performance. The synthesis takes advantage of the methodology developed by the Danishefsky group which allows $C_2$ – alkylation of 3-substituted indoles [32]. In order to avoid possible side reactions in this sensitive step, a phthalyl protecting group was first used for the primary amine of tryptophan which would later be substituted with a Boc group. The rationale behind this choice was that the imide nature of the nitrogen would preclude any possibility of cyclization of the presumed 3-chloroindolenine intermediate **3**.

First, commercially available DL-tryptophan was protected with a phthalyl group based on a literature procedure [33], followed by the introduction of a *tert*-butyl ester by using a similar published protocol [34] to afford the protected intermediate **2** in good yield (67%). Allylation on the C-2 of the protected tryptophan was achieved by following a two step reaction sequence [32]. In the first step, reaction of the protected tryptophan with *tert*-butyl hypochlorite yields presumably the unstable intermediate 3-chloroindolenine **3** which then reacts with allytributyltin and an acidic promoter ($BF_3 \cdot Et_2O$) to yield the compound with the desired structure. With the chosen protecting groups the reaction proceeded efficiently to yield compound **4** in the excellent yield of 97%.

Next the phthalyl group was substituted with a Boc group by a two-step reaction sequence. In the first step the phthalyl group was cleaved with methylhydrazine by heating in benzene at 65 °C for several hours [35]. Attempts to deprotect by using standard hydrazinolysis led to partial reduction of the double bond, possibly through diimide formation in situ, resulting from oxidation of hydrazine with traces of oxygen or any other oxidant [36]. Addition of excess of cyclopentene to the reaction mixture, which can be easily reduced by hydrazine [37] and thus spare the reduction of the allyl functionality, did not efficiently prevent some partial reduction of the allyl moiety. Separation of the reduced byproduct was not possible since both compounds were running exactly at the same $R_f$ on TLC. The use of methylhydrazine on the other hand yielded smoothly the free amine with no side products. The intermediate amine was not isolated but reacted directly with Boc anhydride and triethylamine to yield the *N*-Boc protected amino acid **5** in excellent yield (97%) over two steps.

A second Boc group was then introduced on the nitrogen of the indole ring by reacting **5** with Boc anhydride and catalytic amounts of DMAP to provide compound **6** in 87% yield. The rationale behind the introduction of an electron withdrawing protecting group on the nitrogen of the aromatic core was to remove electron density from the indole ring and reduce the nucleophilicity of C-3 and thus avoid possible side reactions during the following hydroboration/oxidation step. Reaction of the fully *tert*-butyl protected allyl tryptophan **6** with 9-BBN and subsequent oxidation ($NaOH/H_2O_2$) yielded the corresponding alcohol **7** in excellent yield (92%). Clearly, the combination of removing electron density from the indole ring and making use of the bulky 9 – BBN ensured that hydroboration takes place only at the terminal alkene bond. Alcohol **7** was then treated with mesyl chloride to yield the corresponding mesylate **8** in 88% yield which would also be used as the precursor for the radiosynthesis of [$^{18}$F]2-FPTRP later. The mesyl intermediate was consequently reacted with cesium fluoride (CsF) in *tert*-butanol [38] to give fluorinated compound **9** in excellent yield (98%).

Finally, treatment of the fluorinated intermediate with TFA in dichloromethane in the presence of scavengers led to the final compound 2-FPTRP **10** which was purified by preparative HPLC. When the reaction was carried out without the presence of scavengers, HPLC analysis revealed that only 32% of the desired compound was present in the reaction mixture and the rest were byproducts with higher retention times (Fig. 3A). The more lipophilic peaks can be most possibly attributed to *t*-butylation of the highly reactive indole ring during deprotection of the Boc groups. It

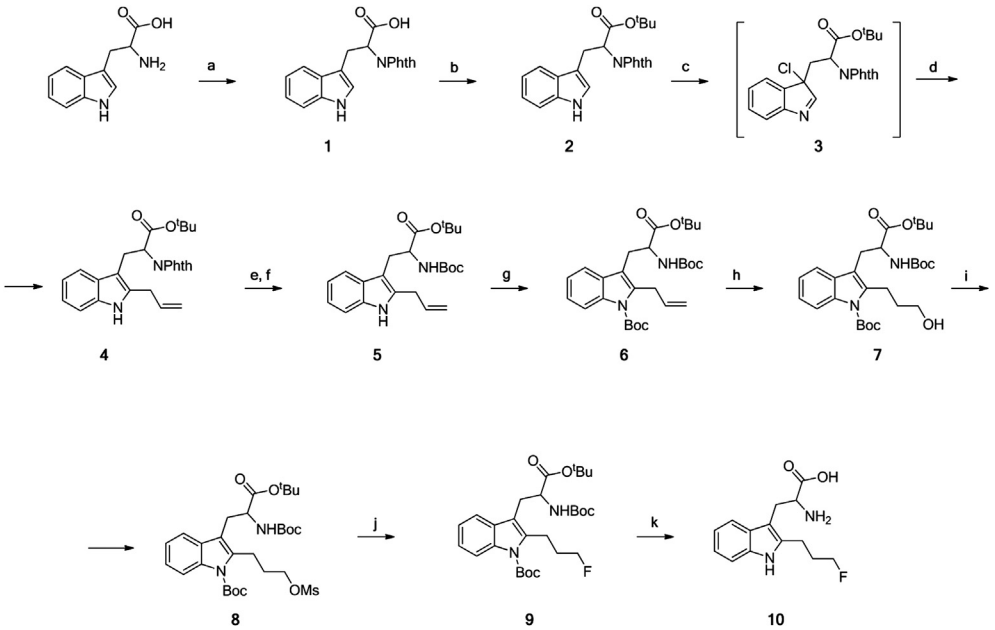


**Scheme 1.** Synthesis of 2-FPTRP and precursor. Reagents and conditions: (a) phthalic anhydride, $Et_3N$, DMF, reflux, 8 h, 97%; (b) *t*-BuBr, TEBAC, $K_2CO_3$, *N*,*N*-DMAC, 55 °C, 2.5 h, 67%; (c) *t*-BuOCl, $Et_3N$, THF −78 °C, 0.5 h; (d) allyltributyltin, $BF_3 \cdot Et_2O$, THF, −78 °C to r.t., 16 h, 97% (2steps); (e) $MeNHNH_2$, benzene, r.t. 6 h, 65 °C 14 h; (f) Boc anhydride, $Et_3N$, DCM, 0 °C to r.t., 2.5 h, 97% (2 steps); (g) Boc anhydride, $DMAP_{(cat)}$, DCM/MeCN (1:1), 0 °C to r.t., 2 h, 87%; (h) 9-BBN, THF, r.t. 4 h then $H_2O$, NaOH 3 M, $H_2O_2$ 30%, r.t., 3 h, 92%; (i) MsCl, $Et_3N$, DCM, 0 °C, 1 h, 88%; (j) CsF, *t*-BuOH, 80 °C, 7 h, 98%; (k) TFA, DCM, $HSCH_2CH_2SH$, $(CH_3)_2S$, 0 °C to r.t. 2 d, 50 °C 1 h, 83%.

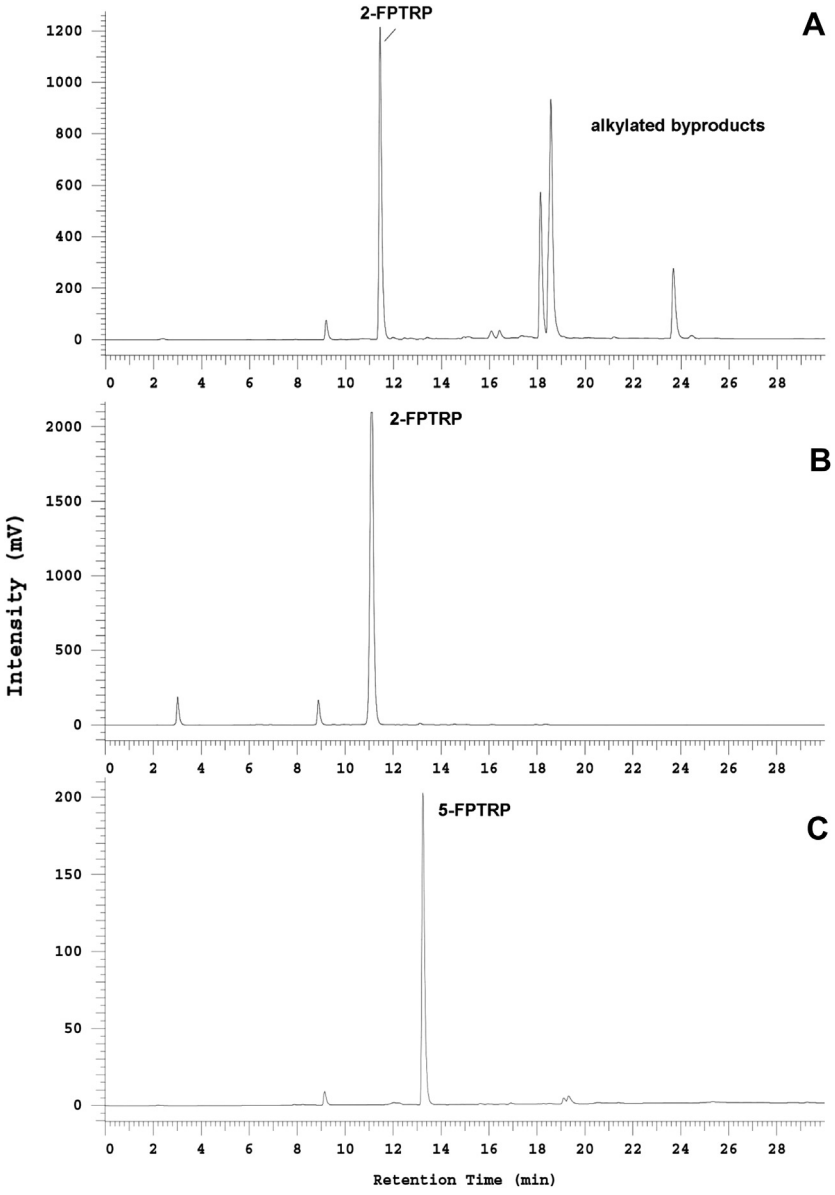


**Fig. 3.** HPLC chromatograms of final TFA deprotection reactions indicating: (A) the presence of more lipophilic by-products without the use of scavengers for 2-FPTRP; (B) a clean reaction with the presence of scavengers for 2-FPTRP; (C) a clean reaction with the presence of scavengers for 5-FPTRP.

is known that acidic cleavage of *t*-Bu and Boc groups results in *t*-butyl cations and *tert*-butyl trifluoroacetate formation and these species are responsible for alkylation of the indole ring of tryptophan [39]. The use of cresol as a scavenger [40] (up to 10 equivalents) did not efficiently suppress alkylation. Nevertheless, when a combination of 1,2 ethanedithiol (10 equivalents) and dimethylsulfide (130 eq) was used [41], the reaction yielded cleanly the free amino acid 2-FPTRP **10** (Fig. 3B).

The synthesis of 5-FPTRP was accomplished following a similar methodology as described for 2-FPTRP and is presented in Scheme 2. Again *t*-butyl based protecting groups were used and the main difference relies on the method employed for incorporating the allyl functionality, which, in this case, was achieved via the Suzuki–Miyaura cross-coupling reaction of a protected 5-bromo tryptophan. In detail, commercially available DL-5-bromo tryptophan was protected with a Boc group [42] and a *tert*-butyl ester [34] with yields 92% and 59% respectively to give compound **12**. Sequentially, a second Boc group was again inserted on the nitrogen of the indole ring as described for 2-FPTRP, to avoid possible side reactions during hydroboration/oxidation reaction. The palladium catalyzed cross coupling reaction of **13** with allylboronic acid pinacol ester [43] afforded the allyl intermediate **14** in very satisfactory yield (82%) which was then subjected under hydroboration/oxidation conditions to yield the corresponding alcohol **15** in 92% yield. Finally, as described in the case of 2-FPTRP, mesylation of the alcohol, followed by fluorination with CsF and triple Boc deprotection with TFA afforded the final compound 5-FPTRP **18** (Fig. 3C).

$^1$H NMR peaks were fully assigned for all new compounds and assignment was based on the combined analysis of a series of $^1$H–$^1$H correlation spectra. The numbering of the atoms is shown in Fig. 2. In the case of 2-FPTRP, the H-7 proton was distinguished from the rest of the aromatic protons on the basis of the presence of a NOE correlation peak with H-1. Having H-7 as a starting point, the rest of the indole protons were assigned according to their correlations in the COSY spectra. The most notable $^1$H NMR shift difference among the various intermediates during the synthesis of 2-

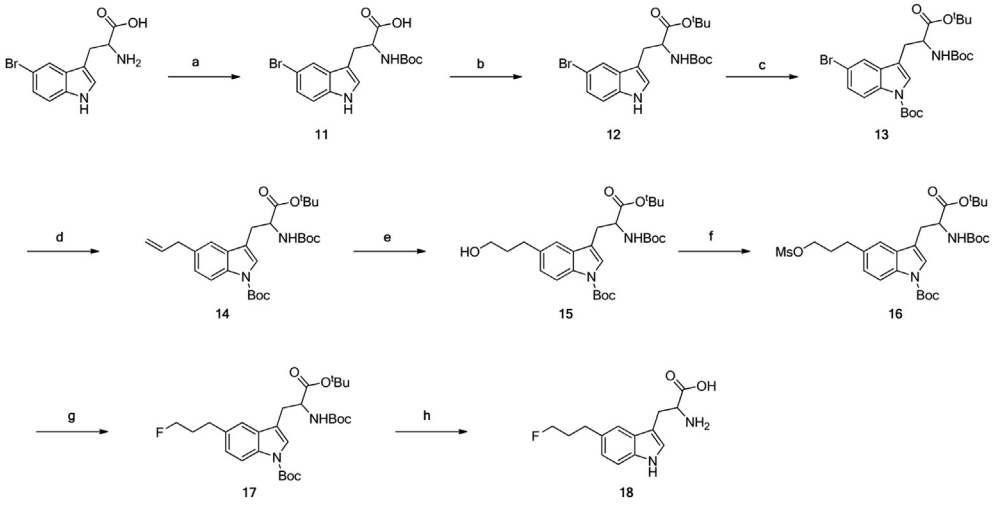

**Scheme 2.** Synthesis of 5-FPTRP and corresponding precursor. Reagents and conditions: (a) Boc anhydride, NaOH, dioxane/water, r.t., 3 h, 92%; (b) *t*-BuBr, TEBAC, $K_2CO_3$, *N*,*N*-DIMAC, 55 °C, 2.5 h, 59%; (c) Boc anhydride, $DMAP_{(cat)}$, DCM/MeCN (1:2), 0 °C to r.t., 2 h 98%; (d) allylboronic acid pinacol ester, CsF, $Pd(PPh_3)_4$, THF, reflux, 16 h, 82%; (e) 9-BBN, THF, r.t. 4 h then $H_2O$, NaOH 3 M, $H_2O_2$ 30%, r.t., 3 h, 92%; (f) MsCl, $Et_3N$, DCM, 0 °C, 1 h, 95%; (g) CsF, *t*-BuOH, 80 °C, 7 h, 93%; (h) TFA, DCM, $HSCH_2CH_2SH$, $(CH_3)_2S$, 0 °C to r.t. 16 h, 50 °C 1 h, 89%.

FPTRP can be seen for compound **6**. The strong electron pull effect which is triggered after the introduction of the Boc group on the nitrogen of the indole ring is reflected in the profound chemical shift difference of all the aromatic protons which appear deshielded by 0.1 (for H-4) to 0.8 (for H-7) ppm compared to compound **5**. An analogous downfield shifting can be observed for almost all the carbons of the indole core (0.1–4.3 ppm difference), with C-3 being deshielded most prominently by 9 ppm. Final reference compounds 2-FPTRP and 5-FPTRP were additionally fully characterized by $^{13}C$ NMR and peaks were assigned by interpretation of a series of $^{1}H-^{13}C$ correlation spectra. The assignment of the ambiguous C-2, C-3, C-3a and C-7a peaks was established through the observation of long range heteronuclear coupling with H-12, H-9, H-5 and H-6 respectively for 2-FPTRP. The $^{1}H$ and $^{13}C$ assignments for 5-FPTRP were performed in a similar manner.

### 2.2. Radiochemistry

[$^{18}F$]2-FPTRP and [$^{18}F$]5-FPTRP were prepared by a two step reaction sequence involving nucleophilic fluorination of fully *tert*-butyl protected mesylate precursors (**8**, **16** respectively) and subsequent deprotection (Scheme 3). Nucleophilic substitution was achieved by heating the corresponding mesylate precursors with [$^{18}F$]TBAF in acetonitrile at 100 °C for 10 min. In our early attempts, continuation of radiosynthesis involved HPLC purification of the [$^{18}F$] labeled intermediates followed by deprotection with HCl 4 M and then neutralization with NaOH 4 M. Unfortunately, quality control of the final product revealed the presence of several more polar radioactive byproducts whose percentage would vary, depending on the amount of the starting activity and speed of manipulations during the synthesis. As a result, the final radiochemical purity of the product in the formulation would usually diverge from 95 to 80% while it decreased with time reaching as low as 70% at 4 h (Fig. 4, A and B). These byproducts most probably originate from oxidation of the indole ring due to radiolysis. It has been shown that tryptophan is particularly radiosensitive since the electron rich indole core is a primary target of oxygen radicals produced during radiolysis leading to hydroxyl derivatives or ring scission [44]. The use of sodium ascorbate in various steps during this procedure did not efficiently stop the formation of these byproducts although its addition at the final formulation would prevent further break down of the molecule.

In order to overcome this problem an alternative methodology was devised which involves purification at the final step. In detail, after nucleophilic substitution, the solvent was removed and HCl 4 M was added to the crude and heated at 100 °C for 10 min. The acidic solution was then carefully neutralized with NaOH 4 M and PBS 0.6 M and injected on the semipreparative HPLC. The product was subsequently collected in a vial containing sodium ascorbate to prevent decomposition by radiolysis. This method has the advantage of reduced synthesis time, and additionally UPLC analysis of the reaction mixture before semi-preparative HPLC purification revealed that there were no polar byproducts present as was the case in the initial methodology. We speculate that the excess of precursor present in the reaction mixture might be acting as a scavenger of active oxygen species formed from radiolysis.

The solutions containing the purified tracers were then carefully neutralized to pH ≈ 6 with 10% sodium hydrogen carbonate solution, diluted with water for injection, passed through a sterile filter and used for biological studies. The identity of the radiolabeled compounds was confirmed by co-injection with the reference compounds **10** (for [$^{18}F$]2-FPTRP) and **18** (for [$^{18}F$]5-FPTRP). Chemical and radiochemical purity of both HPLC purified tracers was examined on analytical RP $C_{18}$ column and were always found to be >99% (Fig. 4C and D for the 2- and 5-analog

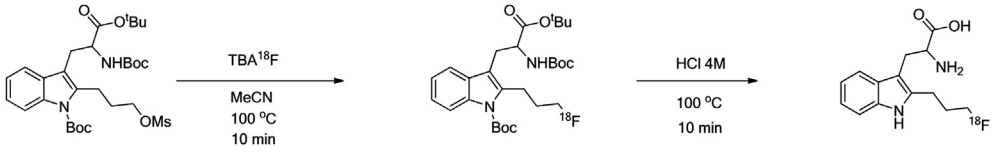

**Scheme 3.** Radiosynthesis of [$^{18}F$]2-FPTRP. Exactly the same methodology and experimental conditions were applied for [$^{18}F$]5-FPTRP.

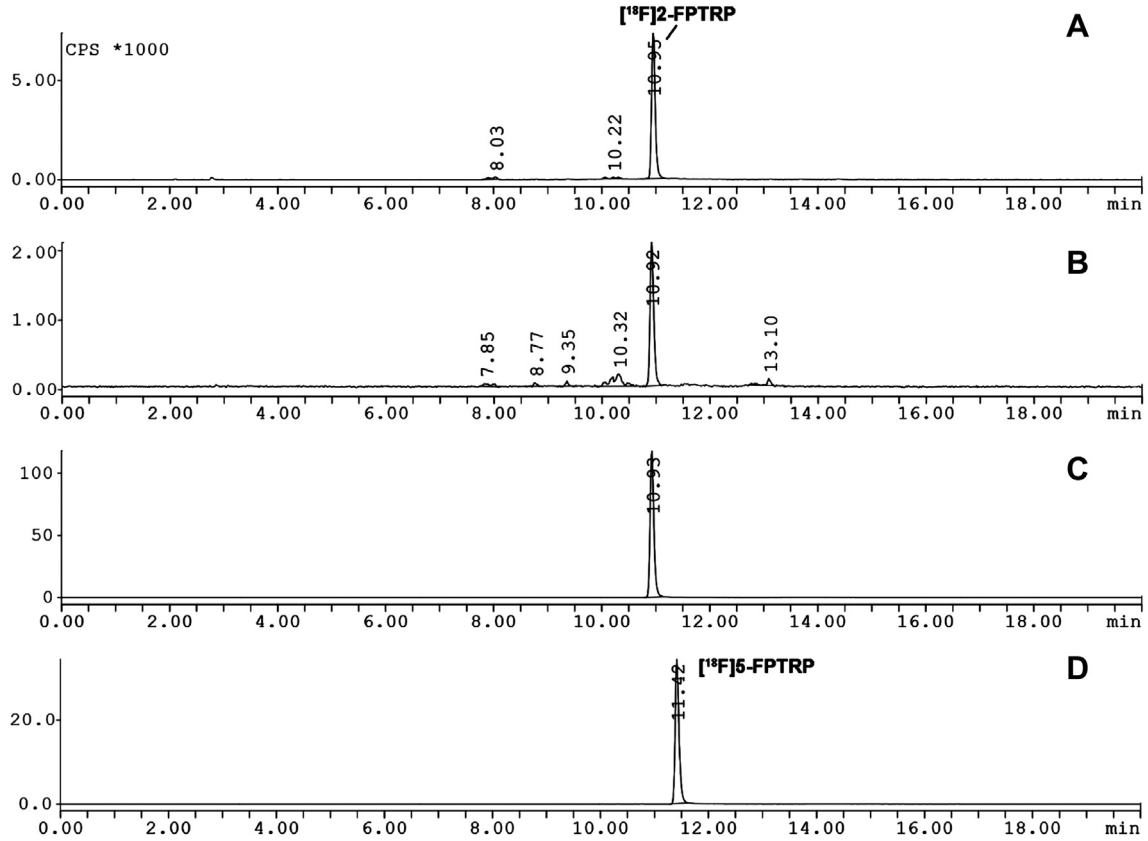


**Fig. 4.** HPLC radio chromatograms of formulated [$^{18}$F]2-FPTRP and [$^{18}$F]5-FPTRP: (A, B) Method involving HPLC purification of the fluorinated protected intermediates, A; $t = 0$, B; $t = 4$ h, [$^{18}$F]2-FPTRP; (C) Method involving HPLC purification as the final step, [$^{18}$F]2-FPTRP; (D) Method involving HPLC purification as the final step, [$^{18}$F]5-FPTRP.

respectively). The products were stable for up to 4 h in this formulation. In a typical experiment, a radiochemical yield of about 34% and 29% (both decay corrected) was achieved for [$^{18}$F]2-FPTRP and [$^{18}$F]5-FPTRP respectively. The specific activities for both tracers were in the range of 30–82 GBq/μmol at the end of synthesis. The total synthesis time from end of bombardment was approximately 90 min.

### 2.3. In vitro cell uptake studies

The uptake of [$^{18}$F]2-FPTRP and [$^{18}$F]5-FPTRP into NCI-H69 cells was studied at 37 and 4 °C (Fig. 5), strictly following the same experimental conditions as in the case of [$^{18}$F]L-FEHTP [24], so as the comparison to be legitimate. Within the first 5 min after addition of [$^{18}$F]2-FPTRP and [$^{18}$F]5-FPTRP, respectively, 49% and

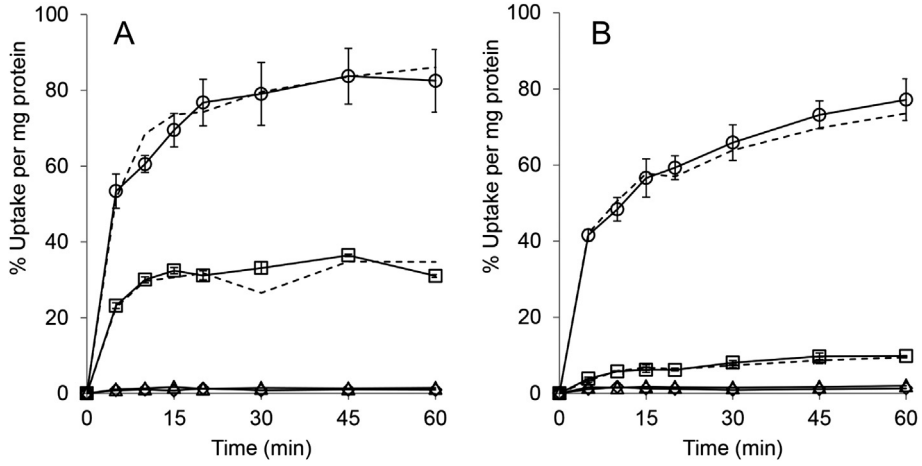


**Fig. 5.** Uptake of [$^{18}$F]2-FPTRP (A) and [$^{18}$F]5-FPTRP (B) into NCI-H69 cells at 37 °C (circles, $n = 3$ from 2 independent experiments, error bars indicate standard deviations) and at 4 °C (squares, $n = 2$ from one experiment, error bars indicate single values). Triangles and diamonds, uptake at 10 mM LAT1/2 inhibitor BCH at 37 °C and 4 °C, respectively ($n = 1$ each). Dotted lines, uptake in the presence of *S*-carbidopa (symbols are not shown for better visibility, $n = 1$ each). Comparing uptake of the two amino acids (in the absence of *S*-carbidopa or BCH), all data except 37 °C 60 min were significantly different ($P$ 0.05).

40% of total added radioactivity accumulated within the cells per mg protein at 37 °C. After the fast initial uptake, radioactivity increased steadily up to 75 and 70%/mg, respectively, within 1 h, reaching equilibration in case of [$^{18}$F]2-FPTRP but not [$^{18}$F]5-FPTRP. The uptake followed the order: [$^{18}$F]2-FPTRP > [$^{18}$F]5-FPTRP > [$^{18}$F]L-FEHTP [24], indicating that substitution of the fluoroethoxy with fluoropropyl side chain could be an efficient approach towards higher tumor accumulation *in vivo*. The uptake of both tracers at 4 °C was lower than at 37 °C but still significant, indicating a facilitated transport mechanism such as transport by LAT. The LAT competitive inhibitor 2-amino-2-norboranecarboxylic acid (BCH 10 mM) reduced both tracers' uptake by more than 97% at 37 °C. Neither 80 μM *S*-carbidopa nor 0.3% DMSO (the vehicle of *S*-carbidopa) had an influence on cell uptake (Fig. 2). These results suggest that transport by LAT is most probably a major uptake route for [$^{18}$F]2-FPTRP and [$^{18}$F]5-FPTRP in NCI-H69 cells.

### 2.4. Small animal PET with xenograft-bearing mice

Based on the favorable uptake kinetics of the [$^{18}$F] labeled propyltryptophans into NCI-H69 cells *in vitro* we examined their uptake into NCI-H69 and PC-3 xenografts *in vivo* and compared the results to those of [$^{18}$F]FET and to the previously described [$^{18}$F]L-FEHTP [24]. Standard uptake value (SUV) ratios between tumor(s) and reference region of all three amino acids studied in this work were highest between 60 and 80 min post injection of tracer (p.i.). The corresponding images are shown in Fig. 6. In both xenograft models, [$^{18}$F]2-FPTRP reached a SUV ratio of 2.4 (one PC-3 xenograft scanned 60 min p.i.; 3 NCI-H69 xenografts scanned 1, 30 and 60 min p.i., average SUV ratio NCI-H69 2.38 ± 0.02). The SUV ratios were remarkably higher than previously described for [$^{18}$F]L-FEHTP (ratios <2 in both models), which was evaluated under the same experimental conditions [24]. The difference was significant for the NCI-H69 xenografts, where $n = 3$ in this study (no statistical analysis for PC-3, as $n = 1$). SUV ratios of [$^{18}$F]FET were lower in the PC-3 xenograft model (2.17 and 2.12 in two animals) but higher in a NCI-H69 xenograft-bearing mouse, i.e., 2.75, all scan starts 60 min p.i. SUV ratios of [$^{18}$F]5-FPTRP were 1.8 in both models (scan start 60 min p.i., one animal each), similar to its ethoxy analog [$^{18}$F]L-FEHTP [24]. These results are in accordance with the observed higher *in vitro* cell uptake for [$^{18}$F]2-FPTRP. [$^{18}$F]2-FPTRP SUVs of NCI-H69 xenograft and reference region were not affected by pre-administration of *S*-carbidopa in one mouse, indicating that decarboxylation was not involved in [$^{18}$F]2-FPTRP accumulation (SUV ratio was 2.42). Faint accumulation of radioactivity in bone was observed after [$^{18}$F]2-FPTRP but not [$^{18}$F]5-FPTRP application (Fig. 6). Compared to [$^{18}$F]5-FPTRP, [$^{18}$F]2-FPTRP shows a remarkably high tumor/background ratio, in the range of [$^{18}$F]FET, a tyrosine analog used in the clinic for tumor imaging.

Stereochemistry is known to affect the transport of many radiolabeled amino acids. While mammalian cells preferentially use the L-enantiomer for their biological needs, both the D- and the L-enantiomers of some natural and non-natural amino acids may be transported [9]. Especially for the LAT type, it has been shown that LAT1 transports certain D-amino acids with high affinity such as D-phenylalanine, D-leucine and D-methionine [12,45] although not all isoforms can tolerate D-amino acids. For example, LAT2 is stereospecific for the L-isomers of the aforementioned amino acids [45]. As a general trend, L-isomers exhibit considerably higher *in vitro* and *in vivo* tumor uptake than their D-isomers as in the case of [$^{18}$F]FET [46]. A few exceptions, however, do exist where the opposite is true as for example *cis*-4-[$^{18}$F]fluoroproline [47].

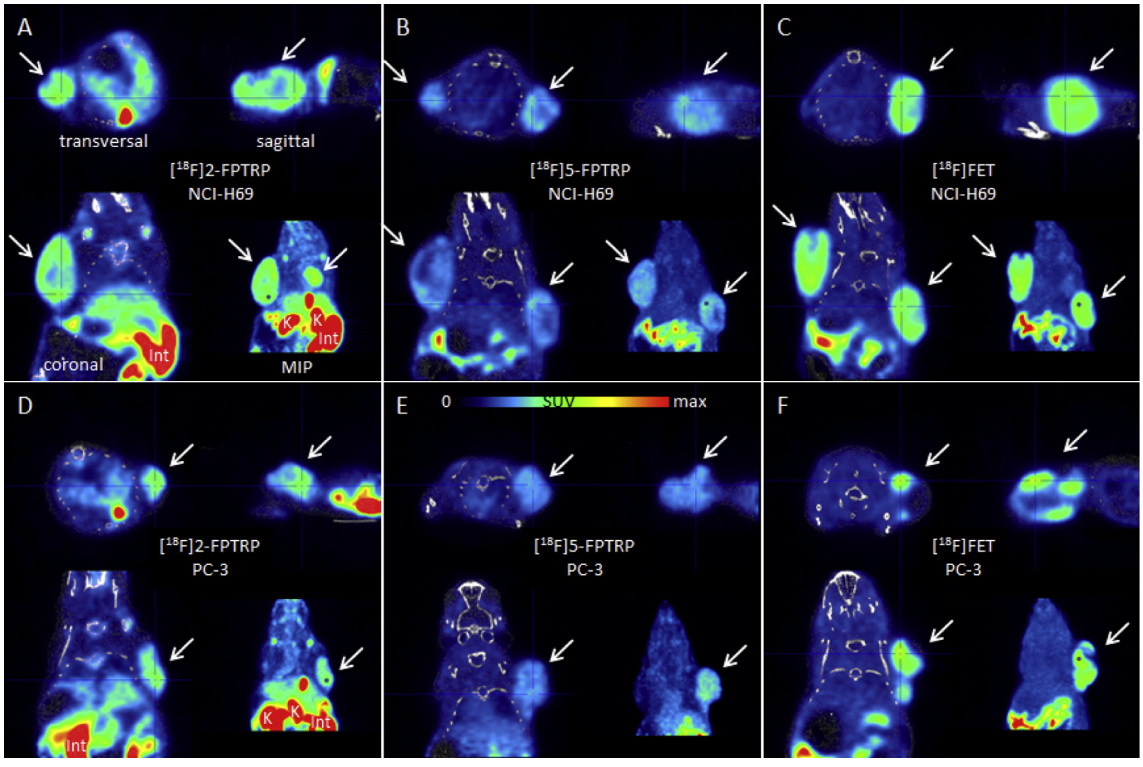


**Fig. 6.** PET/CT images of xenograft-bearing mice. NCI-H69 (A, B, C) and PC-3 (D, E, F) xenograft-bearing mice were injected with 10–14 MBq [$^{18}$F]2-FPTRP (A, D), [$^{18}$F]5-FPTRP (B, E) or [$^{18}$F]FET (C, F) into a tail vein and PET data was acquired between 60 and 150 min p.i. Shown are averaged data between 60 and 80 min p.i., when tumor/reference ratios were highest. Maximal (max) SUVs are 2 (A, D, E), 4 (B) and 5 (C, F), respectively, resulting in similar dark blue background color. CT is shown in gray and white. Arrows, xenografts; MIP, maximal intensity projection; K, kidneys; Int, intestines. Cross hairs indicate optical planes. Anatomical left is left in images. (For interpretation of the references to color in this figure legend, the reader is referred to the web version of this article.)

There are also some examples where the D-isomers show different pharmacokinetics compared to their L-isomers, as a result of their recognition by different transport systems, sometimes leading to interesting imaging properties. For example, biological evaluation of the D-enantiomers of *O*-[$^{18}$F]fluoromethyl-, fluoroethyl- and fluoropropyl tyrosine demonstrated lower overall tumor uptake but higher tumor to blood ratios compared to their L-enantiomers [48]. We were delighted to note that the new racemic tryptophan analogs seem to perform better *in vitro* and *in vivo* than our previously reported [$^{18}$F]L-FEHTP [24], and in addition comparable to the routinely used [$^{18}$F]FET. It is possible that better results could be achieved by comparing enantiomerically pure [$^{18}$F]2-FPTRP and [$^{18}$F]5-FPTRP, and the prospect of undertaking such an approach is currently under evaluation.

### 2.5. Ex vivo metabolite studies

In order to assess whether any biotransformation step is involved in the relatively high tumor uptake of [$^{18}$F]2-FPTRP, we investigated the *in vivo* metabolism of the two tryptophan analogs. Up to 60 min post injection, only intact compound was detected in the plasma for both tracers (data not shown). Based on these results, we excluded a possible involvement of a biotransformation step in tumor accumulation. For comparison, no parent compound was detected in blood 60 min after injection of the AADC substrate [$^{18}$F]FDOPA in the same mouse strain [24]. Apparently, this structural modification on the tryptophan is not tolerated by the AADC enzyme.

## 3. Conclusions

Two new fluoropropyl tryptophan analogs ([$^{18}$F]2-FPTRP) and ([$^{18}$F]5-FPTRP) were prepared in high radiochemical purity, good radiochemical yields and high specific activity. Both compounds accumulate predominantly via LAT transport, showing a higher *in vitro* cell uptake than the previously reported 5-fluoroethoxy analog [$^{18}$F]L-FEHTP. Small animal PET imaging studies in two different xenograft tumor models indicated that [$^{18}$F]2-FPTRP was comparable to the well established [$^{18}$F]FET tracer while [$^{18}$F]5-FPTRP shows slightly lower tumor uptake, similar to [$^{18}$F]L-FEHTP. The fact that radiometabolite studies showed only intact compound in plasma for both tracers and that pre-administration of carbidopa does not seem to influence the *in vivo* imaging with [$^{18}$F]2-FPTRP suggests that a biotransformation step is probably not involved in tumor accumulation. The higher observed tumor uptake for [$^{18}$F]2-FPTRP, compared to [$^{18}$F]5-FPTRP or [$^{18}$F]L-FEHTP could be attributed to its more efficient transport through LAT as indicated by the *in vitro* assays. The results demonstrate that [$^{18}$F]2-FPTRP is a promising PET probe for the LAT activity of malignant lesions, not influenced by AADC activity. It can also be concluded that the 2-position of the indole ring is a promising site for derivatization of tryptophan resulting in favorable tumor-to-background ratios.

## 4. Experimental section

### 4.1. Materials and instrumentation

All reagents and starting materials were purchased from commercial suppliers and used without further purification. *Tert*-butyl hypochlorite was synthesized by following a published protocol [49]. *N*-Phthalyl-DL-tryptophan (**1**) and 5-bromo-*N*-Boc-DL-tryptophan (**11**) were also synthesized as mentioned in the literature with slight modifications [33,42]. All solvents used for reactions were purchased as anhydrous grade from Acros Organics (puriss., dried over molecular sieves, $H_2O$ <0.005%) and were used without further purification unless otherwise stated. Solvents for extractions, column chromatography and thin layer chromatography (TLC) were purchased as commercial grade. All non aqueous reactions were performed under an argon atmosphere using flame-dried glassware and standard syringe/septa techniques. Reactions at 0 °C were carried out in an ice/water bath. Reactions at −78 °C were carried out in a dry ice/acetone bath. In general, reactions were magnetically stirred and monitored by TLC performed on Merck TLC glass sheets (silica gel 60 $F_{254}$). Spots were visualized with UV light ($\lambda = 254$ nm) or through staining with anisaldehyde solution or basic aq. $KMnO_4$ solution and subsequent heating. Chromatographic purification of products was performed using Fluka silica gel 60 for preparative column chromatography (particle size 40–63 μm). Purity of compounds was ≥95% as determined by analytical HPLC method on an Agilent HPLC system.

Nuclear magnetic resonance (NMR) spectra were recorded in $CDCl_3$ or DMSO-$d_6$ on a Bruker Av-400 spectrometer at room temperature. The measured chemical shifts are reported in $\delta$ (ppm) and the residual signal of the solvent was used as the internal standard ($CDCl_3$ $^1$H: $\delta = 7.26$ ppm, $^{13}$C: $\delta = 77.0$ ppm, DMSO-$d_6$: $^1$H: $\delta = 2.50$ ppm, $^{13}$C: $\delta = 39.51$ ppm). For the $^{19}$F NMR spectra, $CFCl_3$(=0.00 ppm) was used as the internal standard. All $^{13}$C NMR spectra were measured with complete proton decoupling. Data of NMR spectra are reported as follows: s = singlet, d = doublet, t = triplet, m = multiplet, dd = doublet of doublets, dt = doublet of triplets, dq = doublet of quartets, dm = doublet of multiplets, br = broad signal. The coupling constant *J* is reported in Hertz (Hz). The numbering of the H and C atoms can be seen in Fig. 3. Electrospray (ES) mass spectra (HRMS) were obtained with a Bruker FTMS 4.7 T BioAPEXII spectrometer. High-performance liquid chromatography (HPLC) was performed on a Merck–Hitachi L-7000 system equipped with an L-7400 tunable absorption detector.

Analytical HPLC was performed with a reverse phase column (Ultimate® XB-C18 column 4.6 × 150 mm, 3 μm) with the following solvent system: water/0.1% TFA (solvent A), acetonitrile (solvent B); 0–30 min: 5–70% B. The flow rate was 1 ml/min and UV detection at 280 nm. Preparative HPLC was performed with a reverse phase preparative column (Ultimate® XB-C18 column 21.2 × 150 mm, 5 μm) using the above mentioned gradient for analytical HPLC at a flow of 20 ml/min. Analytical radio-HPLC was performed on an Agilent 1100 system equipped with multi-UV-wavelength and Raytest Gabi Star detectors and Gina Star software. A reverse phase column was used (LiChrospher® 100 RP-18 5 μm LiChroCART® 4 × 250 mm) with the following solvent system: $H_2O$ (0.1% TFA) (solvent A), acetonitrile (solvent B); flow 1 mL/min; 0–3 min: 5% B, 3–20 min: 5–90% B, 20–25 min: 90% B, 25–27: 90–5% B, 27–30 min 5% B; UV = 280 nm. Semipreparative purification of radiolabeled material was performed on a Merck–Hitachi L6200A system equipped with Knauer variable wavelength detector and an Emberline radiation detector using a reverse phase column (Phenomenex Luna C18, 10 × 250 mm, 5 μm) and isocratic conditions consisting of 8% EtOH in 35 mM acetate buffer (pH ≈ 4) at a flow rate of 4 ml/min (UV = 280 nm). For reaction monitoring during radiosynthesis and for the metabolite studies a Waters Ultra-performance liquid chromatography (UPLC®) system was used with an Acquity UPLC BEH C18 column (2.1 × 50 mm, 1.7 μm, Waters) and an attached coincidence detector (FlowStar LBS13, Berthold). The mobile phase consisted of the following system: $H_2O$ (0.1% TFA) (solvent A), acetonitrile (solvent B); flow 0.6 mL/min; 0–0.3 min: 0% B, 0.3–2.2 min: 0–70% B, 2.2–2.6 min: 70% B, 2.6–3.0 min: 70–0% B; UV = 280 nm.

Purity of biologically tested compounds ([$^{18}$F]2-FPTRP and [$^{18}$F]5-FPTRP) was ≥99% as determined by the aforementioned analytical radio-HPLC method. Specific activity was calculated by comparing ultraviolet peak intensity of final formulated products

with calibration curves of corresponding non-radioactive standards of known concentrations.

### 4.2. Chemistry

#### 4.2.1. Tert-butyl 2-(1,3-dioxoisoindolin-2-yl)-3-(1H-indol-3-yl) propanoate (**2**)

A mixture of *N*-phthalyl protected tryptophan **1** (15.8 g, 47.3 mmol), potassium carbonate (32.7 g, 236 mmol) and triethylbenzylammonium chloride (TEBAC) (10.76 g, 47.3 mmol) was suspended in *N*,*N*-dimethylacetamide (47 ml). A mechanical stirrer was used for efficient stirring and to this suspension *tert*-butyl bromide (64.8 g, 473 mmol) was added and the mixture was heated for 2.5 h at 55 °C. The reaction was then poured to a funnel containing cold water (350 ml) and extracted with ethyl acetate (3 × 250 ml). The combined organic layers were washed with brine (1 × 300 ml), dried over sodium sulfate, filtered and evaporated to dryness under reduced pressure. The crude was purified with flash column chromatography using hexane/ethyl acetate 8:2 to yield 12.4 g (67%) of a white powder. $^1$H NMR ($d_6$-DMSO, 400 MHz) $\delta$ 10.75 (br, 1H, H-1), 7.83–7.80 (m, 4H, N*Phth*), 7.50–7.45 (m, 1H, H-4), 7.27–7.22 (m, 1H, H-7), 7.04 (d, $^3J_{H2-H1}$ = 2.4 Hz, 1H, H-2), 7.02–6.96 (m, 1H, H-6), 6.91–6.86 (m, 1H, H-5), 5.01 (dd, $^3J_{H9-H8a}$ = 9 Hz, $^3J_{H9-H8b}$ = 6.8 Hz, 1H, H-9), 3.56–3.49 (m, 2H, H-8), 1.39 (s, 9H, C(C$H_3$)$_3$–*t*-butyl ester). $^{13}$C NMR ($d_6$-DMSO, 100 MHz) $\delta$: 167.7, 167.1, 136.0, 134.8, 130.8, 126.9, 123.5, 123.3, 120.9, 118.3, 117.9, 111.4, 109.5, 81.8, 53.2, 27.5, 24.2. ESI-QTOF MS *m*/*z* calculated for $C_{23}H_{22}N_2O_4$ $[M + Na]^+$ 413.1472, measured 413.1467.

#### 4.2.2. Tert-butyl3-(2-allyl-1H-indol-3-yl)-2-(1,3-dioxoisoindolin-2-yl)propanoate (**4**)

*Tert*-butylhypochlorite (1.67 g, 15.37 mmol) was added dropwise within 10 min to a solution of **2** (5 g, 12.81 mmol) and triethylamine (1.56 g, 15.37 mmol) in THF (64 ml) at −78 °C. The reaction was stirred for 30 min at this temperature and then allyltributyltin (8.48 g, 25.6 mmol) was added, followed by the addition of $BF_3 \cdot Et_2O$ (3.25 ml, 25.6 mmol) and the reaction mixture was allowed to reach room temperature, slowly overnight. After 16 h of stirring, the reaction was quenched by adding 20 ml of sat. $NaHCO_3$ solution at 0 °C, diluted with water and extracted with ethyl acetate. The organic layers were combined and washed with sat. $NaHCO_3$ and then saturated KF solution. The emulsion thus formed was filtered over Celite, rinsed with ethyl acetate, the filtrate and rinsings were combined and washed again with saturated KF solution, followed by water and brine. The organic phase was then dried over sodium sulfate, filtered and concentrated under vacuum. The crude was chromatographed on silica gel using hexane/ethyl acetate 8:2 to afford a bright yellow solid (5.3 g, 97%). $^1$H NMR ($d_6$-DMSO, 400 MHz) $\delta$ 10.65 (s, 1H, H-1), 7.80 (br, 4H, N*Phth*), 7.39–7.34 (m, 1H, H-4), 7.19–7.15 (m, 1H, H-7), 6.95–6.88 (m, 1H, H-5), 6.84–6.78 (m, 1H, H-6), 5.86–5.74 (m, 1H, H-12), 5.04 (dd, $^3J_{H9-H8a}$ = 9.5 Hz, $^3J_{H9-H8b}$ = 6.1 Hz, 1H, H-9), 4.93 (dq, $^3J_{H13b-H12}$-trans = 17.1 Hz, $^2J_{H13b-H13a}$-gem = $^4J_{H13b-H11}$-allyl = 1.5 Hz, 1H, H-13b), 4.84 (dq, $^3J_{H13a-H12}$-cis = 10.0 Hz, $^2J_{H13a-H13b}$-gem = $^4J_{H13a-H11}$-allyl = 1.5 Hz, 1H, H-13a), 3.49–3.43 (m, 2H, H-8), 3.38–3.33 (m, 2H, H-11), 1.39 (s, 9H, C(C$H_3$)$_3$–*t*-butyl ester). $^{13}$C NMR ($d_6$-DMSO, 100 MHz) $\delta$: 167.6, 167.1, 135.3 (2C by HSQC/HMBC), 134.8, 134.5, 130.8, 127.8, 123.2, 120.3, 118.2, 117.3, 115.9, 110.7, 105.5, 81.7, 52.9, 29.9, 27.5, 23.2. ESI-QTOF MS *m*/*z* calculated for $C_{26}H_{26}N_2O_4$ $[M + K]^+$ 469.1524, measured 469.1538.

#### 4.2.3. Tert-butyl 3-(2-allyl-1H-indol-3-yl)-2-((tert-butoxycarbonyl) amino)propanoate (**5**)

To a solution of **4** (0.5 g, 1.16 mmol) in benzene (11.6 ml) was added methylhydrazine (0.54 g, 11.62 mmol) and the solution was stirred for 6 h at room temperature, at which point precipitation of a white solid occurred. The reaction was stirred for 2 more hours and methylhydrazine was added again (0.27 g, 5.81 mmol) and the reaction was heated at 65 °C for 14 h. After cooling, the precipitate was filtered off, washed with benzene (3 × 10 ml) and the combined washings and filtrate were evaporated to dryness under reduced pressure to yield yellowish oil. The free amine was dried under high vacuum for 2 h and used directly for the second step without further purification. The crude intermediate was then dissolved in dichloromethane (9 ml), cooled to 0 °C, triethylamine was added (0.24 g, 2.33 mmol) followed by the addition of a solution of Boc anhydride (0.51 g, 2.33 mmol) in dichloromethane (2.7 ml). The reaction mixture was warmed to room temperature and stirred for 2.5 h, diluted with dichloromethane (40 ml) and washed with water (2 × 25 ml) and brine (1 × 30 ml), dried over sodium sulfate, filtered and concentrated *in vacuo*. The crude product was purified by flash column chromatography using hexane/ethyl acetate 9:1 to yield compound **5** as a yellowish sticky solid (449 mg, 97% over two steps). $^1$H NMR ($d_6$-DMSO, 400 MHz) $\delta$ 10.71 (s, 1H, H-1), 7.49–7.43 (m, 1H, H-4), 7.29–7.22 (m, 1H, H-7), 7.08 (d, $J$ = 8.1 Hz, 1H, N*H*Boc), 7.03–6.96 (m, 1H, H-6), 6.96–6.90 (m, 1H, H-5), 6.02–5.9 (m, 1H, H-12), 5.12 (dq, $^3J_{H13b-H12}$-trans = 17.1 Hz, $^2J_{H13b-H13a}$-gem = $^4J_{H13b-H11}$-allyl = 1.7 Hz, 1H, H-13b), 5.06 (dq, $^3J_{H13a-H12}$-cis = 10 Hz, $^2J_{H13a-H13b}$-gem = $^4J_{H13a-H11}$-allyl = 1.7 Hz, 1H, H-13a), 4.09–3.99 (m, 1H, H-9), 3.52–3.44 (m, 2H, H-11), 3.05 (dd, $^2J_{H8a-H8b}$-gem = 14.4 Hz, $^3J_{H8a-H9}$-vic = 5.8 Hz, 1H, H-8a), 2.93 (dd, $^2J_{H8b-H8a}$-gem = 14.4 Hz, $^3J_{H8b-H9}$-vic = 8.8 Hz, 1H, H-8b), 1.33 (s, 9H, C(C$H_3$)$_3$–*t*-butyl ester), 1.28 (s, 9H, C(C$H_3$)$_3$–NH*Boc*). $^{13}$C NMR ($d_6$-DMSO, 100 MHz) $\delta$: 171.5, 155.3, 135.8, 135.4, 134.4, 128.2, 120.2, 118.1, 117.8, 116.0, 110.6, 106.5, 88.0, 77.9, 55.5, 30.1, 28.1, 27.5, 25.9. ESI-QTOF MS *m*/*z* calculated for $C_{23}H_{32}N_2O_4$ $[M + Na]^+$ 423.2254, measured 423.2244.

#### 4.2.4. Tert-butyl 2-allyl-3-(3-(tert-butoxy)-2-((tert-butoxycarbonyl)amino)-3-oxopropyl)-1H-indole-1-carboxylate (**6**)

To an ice cold solution of **5** (0.43 g, 1.07 mmol) in a mixture of acetonitrile (5.3 ml) and dichloromethane (3.3 ml) was added DMAP (13.1 mg, 0.11 mmol) followed by the addition of a solution of Boc anhydride (245 mg, 1.12 mmol) in dichloromethane (2 ml). After 10 min of stirring, cooling was removed and it was stirred at room temperature for 2 h. The reaction was then diluted with 50 ml dichloromethane, washed with water (2 × 30 ml) and brine (1 × 40 ml), dried over sodium sulfate, filtered and evaporated to dryness under *vacuo*. The crude was purified by flash column chromatography using hexane/ethyl acetate 95:5 to yield a waxy white solid (464 mg, 87%). $^1$H NMR ($d_6$-DMSO, 400 MHz) $\delta$ 8.04–7.97 (m, 1H, H-7), 7.60–7.53 (m, 1H, H-4), 7.29–7.17 (m, 3H, N*H*Boc, H-5, H-6), 6.05–5.91 (m, 1H, H-12), 5.04–4.98 (m, 1H, H-13a), 4.96–4.87 (m, 1H, H-13b), 4.10–3.96 (m, 1H, H-9), 3.86–3.66 (m, 2H, H-11), 3.06 (dd, $^2J_{H8a-H8b}$ gem = 14.6 Hz, $^3J_{H8a-H9}$-vic = 5.8 Hz, 1H, H-8a), 2.97 (dd, $^2J_{H8b-H8a}$-gem = 14.6 Hz, $^3J_{H8b-H9}$-vic = 9.1 Hz, 1H, H-8b), 1.61 (s, 9H, C(C$H_3$)$_3$–Boc indole), 1.31 (s, 9H, C(C$H_3$)$_3$–*t*-butyl ester), 1.30 (s, 9H, C(C$H_3$)$_3$–NH*Boc*). $^{13}$C NMR ($d_6$-DMSO, 100 MHz) $\delta$: 171.0, 155.3, 149.6, 136.0, 135.3, 135.0, 129.3, 123.7, 122.4, 118.5, 115.6, 115.2, 114.8, 83.8, 80.4, 78.1, 54.7, 29.9, 28.1, 27.6, 27.4, 25.5. ESI-QTOF MS *m*/*z* calculated for $C_{28}H_{40}N_2O_6$ $[M + Na]^+$ 523.2779, measured 523.2765.

#### 4.2.5. Tert-butyl 3-(3-(tert-butoxy)-2-((tert-butoxycarbonyl) amino)-3-oxopropyl)-2-(3-hydroxypropyl)-1H-indole-1-carboxylate (**7**)

To a solution of **6** (449 mg, 0.9 mmol) in THF (8.2 ml) was added 9-BBN (0.5 M solution in THF, 2.5 ml, 1.26 mmol) and the clear colorless solution was stirred for 3 h at room temperature. The reaction mixture was then cooled at 0 °C and water (0.46 ml) was

added slowly, followed by the addition of NaOH 3 M (0.47 ml). Subsequently, $H_2O_2$ 30% (0.43 ml) was added carefully within 10 min and then the reaction mixture was allowed to reach room temperature where it was stirred for 3.5 h. The reaction was then partitioned between ethyl acetate and water; the aqueous layer was separated and extracted 3 times with ethyl acetate. The combined organic layers were washed once with brine, dried over sodium sulfate, filtered and evaporated under vacuum. The crude was purified with flash column chromatography using hexane/ethyl acetate 7:3 to yield a colorless oil which solidified to a white solid upon standing at room temperature (430 mg, 92%). $^1$H NMR ($d_6$-DMSO, 400 MHz) $\delta$ 8.05–7.96 (m, 1H, H-7), 7.56–7.51 (m, 1H, H-4), 7.27–7.16 (m, 3H, N*H*Boc, H-5, H-6), 4.50 (t, $^3J_{H13-OH} = 5.1$ Hz, 1H, –$CH_2O$*H*), 4.10–3.97 (m, 1H, H-9), 3.43 (dt, $^3J_{H13-OH} = 5.1$ Hz, $^3J_{H13-H12} = 6.4$ Hz, 2H, H-13), 3.10–2.89 (m, 4H, H-8, H-11), 1.74–1.66 (m, 2H, H-12), 1.63 (s, 9H, C(C*H*$_3$)$_3$ Boc-indole), 1.31 (s, 9H, C(C*H*$_3$)$_3$–*t*-butyl ester) 1.28 (s, 9H, C(C*H*$_3$)$_3$–NH*Boc*). $^{13}$C NMR ($d_6$-DMSO, 100 MHz) $\delta$ 171.1, 155.4, 149.8, 138.1, 135.5, 129.5, 123.5, 122.5, 118.4, 115.0, 114.8, 83.8, 80.4, 78.2, 60.4, 54.8, 33.0, 28.1, 27.7, 27.5, 25.7, 22.8. ESI-QTOF MS *m*/*z* calculated for $C_{28}H_{42}N_2O_7$ $[M + H]^+$ 519.3065, measured 519.3066.

#### 4.2.6. Tert-butyl 3-(3-(tert-butoxy)-2-((tert-butoxycarbonyl) amino)-3-oxopropyl)-2-(3-((methylsulfonyl)-oxy)propyl)-1H-indole-1-carboxylate (**8**)

Mesyl chloride (139 mg, 1.22 mmol) was added dropwise within 5 min to an ice cold solution of **7** (420 mg, 0.81 mmol) and triethylamine (246 mg, 2.43 mmol) in dichloromethane (7.7 ml) and the slight yellow solution was stirred for 1 h at 0 °C. After this time, the reaction was diluted with DCM and washed with saturated $NaHCO_3$ solution (×1), water (×1) and brine, dried over sodium sulfate, filtered and concentrated to dryness under vacuum. The crude was purified with flash column chromatography using hexane/ethyl acetate 8:2 to yield the product as a white flaky solid (425 mg, 88%). $^1$H NMR ($d_6$-DMSO, 400 MHz) $\delta$ 8.05–7.97 (m, 1H, H-7), 7.58–7.51 (m, 1H, H-4), 7.30–7.18 (m, 3H, N*H*Boc, H-5, H-6), 4.25 (t, $^3J_{H13-H12} = 6.2$ Hz, 2H, H-13), 4.09–3.97 (m, 1H, H-9), 3.18 (s, 3H, C*H*$_3$S(=O)$_2$O–), 3.15–2.90 (m, 4H, H-8, H-11), 2.05–1.87 (m, 2H, H-12), 1.64 (s, 9H, C(C*H*$_3$)$_3$ Boc-indole), 1.30 (s, 18H, C(C*H*$_3$)$_3$–*t*-butyl ester/NH*Boc*). $^{13}$C NMR ($d_6$-DMSO, 100 MHz) $\delta$: 171.0, 155.3, 149.7, 136.7, 135.4, 129.3, 123.7, 122.5, 118.4, 115.4, 115.1, 84.0, 80.5, 78.1, 69.7, 54.6, 36.6, 29.1, 28.1, 27.6, 27.4, 25.7, 22.4. ESI-QTOF MS *m*/*z* calculated for $C_{29}H_{44}N_2O_9S$ $[M + Na]^+$ 619.2660, measured 619.2655.

#### 4.2.7. Tert-butyl 3-(3-(tert-butoxy)-2-((tert-butoxycarbonyl) amino)-3-oxopropyl)-2-(3-fluoropropyl)-1H-indole-1-carboxylate (**9**)

A suspension of mesylate **8** (200 mg, 0.34 mmol) and cesium fluoride (255 mg, 1.68 mmol) in *t*-BuOH (1.2 ml) was heated at 80 °C for 7 h at which time TLC confirmed the full consumption of starting material. The reaction mixture was then partitioned between ethyl acetate (30 ml) and water (15 ml), the organic layer was separated and washed again with water (15 ml) and brine (15 ml), dried over sodium sulfate, filtered and evaporated to dryness. The reaction was purified with flash column chromatography using hexane/ethyl acetate to yield a colorless oil (171 mg, 98%). $^1$H NMR ($d_6$-DMSO, 400 MHz) $\delta$ 8.05–7.98 (m, 1H, H-7), 7.59–7.52 (m, 1H, H-4), 7.30–7.18 (m, 3H, N*H*Boc, H-5, H-6), 4.48 (dt, $^2J_{H13-F} = 47.6$ Hz, $^3J_{H13-H12} = 5.9$ Hz, 2H, H-13), 4.09–3.98 (m, 1H, H-9), 3.17–2.89 (m, 4H, H-8, H-11), 2.04–1.81 (m, 2H, H-12), 1.63 (s, 9H, C(C*H*$_3$)$_3$ Boc-indole), 1.31–1.30 (two singlets, 18H, C(C*H*$_3$)$_3$–*t*-butyl ester/NH*Boc*). $^{13}$C NMR ($d_6$-DMSO, 100 MHz) $\delta$: 171.0, 155.3, 149.7, 137.0, 135.4, 129.3, 123.7, 122.5, 118.4, 115.3, 115.1, 83.9, 83.2 (d, $^1J_{C-F} = 162.9$ Hz), 80.4, 78.1, 54.7, 30.4 (d, $^2J_{C-F} = 19.5$ Hz), 28.1, 27.6, 27.4, 25.6, 22.1 (d, $^3J_{C-F} = 5.2$ Hz). $^{19}$F NMR ($d_6$-DMSO, 376 MHz) $\delta$: –217.6 to –218.1 (m). ESI-QTOF MS *m*/*z* calculated for $C_{28}H_{41}FN_2O_6$ $[M + H]^+$ 521.3021, measured 521.3015.

#### 4.2.8. 2-Amino-3-(2-(3-fluoropropyl)-1H-indol-3-yl)propanoic acid (**10**)

TFA (1.7 ml, 22.47 mmol) was added dropwise to an ice cold mixture of compound **9** (90 mg, 0.173 mmol), dimethylsulfane (1.7 ml, 23.34 mmol) and ethane-1,2-dithiol (0.174 ml, 2.07 mmol) in dichloromethane (1. 7 ml). The reaction was stirred for 10 min at 0 °C and then was allowed to reach room temperature where it was stirred for 2 days. The reaction was being monitored by HPLC (2-FPTRP, $t_R = 11.1$ min) After this time, the reaction was heated at 50 °C for 1 h and then the volatiles were removed under reduced pressure. The oil that remained was taken up in water (12 ml), washed with ether (3 × 6 ml) and then concentrated to an approximate volume of 3 ml and the mixture was purified with preparative HPLC. The product eluted approximately at 10.6 min and was obtained as a white solid after lyophilization (38 mg, 83%). $^1$H NMR ($d_6$-DMSO, 400 MHz) $\delta$ 10.85 (s, 1H, H-1), 7.53–7.48 (m, 1H, H-4), 7.29–7.24 (m, 1H, H-7), 7.03–6.97 (m, 1H, H-6), 6.96–6.90 (m, 1H, H-5), 4.46 (dt, $^2J_{H13-F} = 47.5$ Hz, $^3J_{H13-H12} = 6.1$ Hz, 2H, H-13), 3.38 (dd, $^3J_{H8a-H9} = 9.1$ Hz, $^3J_{H8b-H9} = 4.4$ Hz, 1H, H-9), 3.27 (dd, $^2J_{H8b-H8a} = 14.9$ Hz, $^3J_{H8b-H9} = 4.4$ Hz, 1H, H-10b), 2.93–2.76 (m, 3H, H-10a and H-13), 2.09–1.94 (m, 2H, H-12). $^{13}$C NMR ($d_6$-DMSO, 100 MHz) $\delta$: 170.1 (C-10), 136.7 (C-2), 135.7 (C-7a), 128.0 (C-3a), 120.2 (C-6), 118.2 (C-5), 117.8 (C-4), 110.5 (C-7), 105.9 (C-3), 83.4 (d, $^1J_{C13-F} = 162$ Hz, C-13), 55.6 (C-9), 30.0 (d, $^2J_{C12-F} = 19.2$ Hz, C-12), 26.6 (C-8), 21.2 (d, $^3J_{C11-F} = 6.4$ Hz, C-11). $^{19}$F NMR ($d_6$-DMSO, 376 MHz) $\delta$: –217.8 to –218.3 (m). ESI-QTOF MS *m*/*z* calculated for $C_{14}H_{17}FN_2O_2$ $[M + H]^+$ 265.1347, measured 265.1346.

#### 4.2.9. Tert-butyl 3-(5-bromo-1H-indol-3-yl)-2-(tert-butoxycarbonylamino)propanoate (**12**)

A mixture of *N*-Boc protected 5-bromo tryptophan **11** (2.23 g, 5.82 mmol), potassium carbonate (4.02 g, 29.1 mmol) and TEABC (1.33 g, 5.82 mmol) was suspended in *N*,*N*-Dimethylacetamide (1.3 ml). To this suspension, *tert*-butyl bromide (6.5 ml, 58.2 mmol) was added and the mixture was heated for 2 h at 55 °C. After cooling, cold water was added (50 ml) and extracted with ethyl acetate (3 × 40 ml). The combined organic layers were washed once with water and brine, dried over sodium sulfate, filtered and the solvent was evaporated to dryness under reduced pressure. The crude was purified by flash column chromatography on silica gel with hexane/ethyl acetate 8:2 to provide **12** (1.51 g, 59%) as a light yellow solid. $^1$H NMR ($CDCl_3$, 400 MHz) $\delta$ 8.15 (br, 1H, H-1), 7.72 (d, $^4J_{H4-H6} = 1.8$ Hz, 1H, H-4), 7.25 (dd, $^3J_{H6-H7} = 8.5$ Hz, $^4J_{H6-H4} = 1.8$ Hz, 1H, H-6), 7.20 (d, $^3J_{H7-H6} = 8.5$ Hz 1H, H-7), 7.02 (br, 1H, H-2), 5.09 (d, $J = 7.8$ Hz, N*H*Boc), 4.57–4.46 (m, 1H, H-9), 3.28–3.12 (m, 2H, H-8), 1.44 (s, 9H, C(C*H*$_3$)$_3$–*t*-butyl ester), 1.39 (s, 9H, C(C*H*$_3$)$_3$–NH*Boc*). $^{13}$C NMR ($CDCl_3$, 100 MHz) $\delta$: 171.1, 155.1, 134.6, 129.7, 125.0, 123.9, 121.8, 112.9, 112.5, 110.6, 82.1, 79.8, 54.7, 28.3, 27.9 (2 carbons by HSQC). ESI-QTOF MS *m*/*z* calculated for $C_{20}H_{27}BrN_2O_4$ $[M + H]^+$ 439.1227, measured 439.1221.

#### 4.2.10. Tert-butyl-5-bromo-3-(3-tert-butoxy-2-(tert-butoxycarbonylamino)-3-oxopropyl)-1H-indole-1-carboxylate (**13**)

To solution of **12** (0.5 g, 1.14 mmol) in a mixture of acetonitrile (10 ml) and dichloromethane (18 ml) was added DMAP (14 mg, 0.11 mmol) followed by the addition of a solution of Boc anhydride (261 mg, 1.19 mmol) in dichloromethane (2.4 ml) and the reaction mixture was stirred at room temperature for 2 h. The reaction was then diluted with 50 ml dichloromethane, washed with water (2 × 30 ml) and brine (1 × 40 ml), dried over sodium sulfate, filtered and evaporated to dryness under *vacuo*. The crude was purified by

flash column chromatography using hexane/ethyl acetate 9:1 to yield the title compound as waxy white solid (622 mg, 98%). $^1$H NMR ($CDCl_3$, 400 MHz)) $\delta$ 8.00 (br, 1H, H-7), 7.65 (d, $^4J_{H4-H6}$ = 2.0 Hz, 1H, H-4), 7.41–7.36 (m, 2H, H-2 and H-6), 5.13 (d, $J$ = 7.6 Hz, 1H, N*H*Boc, 4.56–4.48 (m, 1H, H-9), 3.21 (dd, $^2J_{H8a-H8b}$ = 14.9 Hz, $^3J_{H8a-H9}$ 1H, H-8a), 3.10 (dd, $^2J_{H8a-H8b}$ = 14.9 Hz, $^3J_{H8a-H9}$ 1H, H-8b), 1.64 (s, 9H, C(C*H*$_3$)$_3$–N*Boc* indole), 1.45 (s, 9H, C(C*H*$_3$)$_3$–*t*-butyl ester), 1.42 (s, 9H, C(C*H*$_3$)$_3$–NH*Boc*). $^{13}$C NMR ($CDCl_3$, 100 MHz) $\delta$: 170.6, 155.0, 149.1, 134.0, 132.6, 127.2, 125.2, 122.0, 116.6, 116.0, 114.8, 83.9, 82.4, 79.8, 54.2, 28.3, 28.1, 27.9, 27.6. ESI-QTOF MS $m/z$ calculated for $C_{25}H_{35}Br\,N_2O_6$ $[M + Na]^+$ 561.1570, measured 561.1571.

#### 4.2.11. Tert-butyl-5-allyl-3-(3-tert-butoxy-2-(tert-butoxycarbonylamino)-3-oxopropyl)-1H-indole-1-carboxylate (**14**)

Cesium fluoride (135 mg, 0.89 mmol) and palladium tetrakis(triphenylphosphine) (51 mg, 44.5 μmol) were added to a solution of **13** (240 mg, 4.45 mmol) in degassed (freeze pump and thaw) tetrahydrofuran (25 ml) and the mixture was stirred for 40 min. Allylboronic acid pinacol ester (0.29 ml, 1.56 mmol) was then added and the system was refluxed for 16 h. After cooling down, the reaction was partitioned between water (30 ml) and ether (30 ml). The organic layer was removed and the aqueous layer was washed twice with ether (20 ml). The combined organic layers were washed with water and brine, dried over sodium sulfate, filtered and the solvent was removed under reduced pressure. The crude was purified by flash column chromatography on silica with hexane/ethyl acetate 92:8 to provide 205 mg (82%) of the product as a white solid. $^1$H NMR ($CDCl_3$, 400 MHz) $\delta$ 8.04 (br, 1H, H-7), 7.39 (br, 1H, H-2), 7.34 (br, 1H, H-4), 7.15 (dd, $J_1$ = 8.5 Hz, $J_2$ = 1.5 Hz, 1H, H-6), 6.07–5.95 (m, 1H, H-12), 5.15–5.03 (m, 3H, H-13 and N*H*Boc), 4.59–4.50 (m, 1H, H-9), 3.52–3.44 (m, 2H, H-11), 3.20 (dd, $^2J_{H8a-H8b}$ = 14.9 Hz, $^3J_{H8a-H9}$ = 5.5 Hz, 1H, H-8a), 3.13 (dd, $^2J_{H8b-H8a}$ = 14.9 Hz, $^3J_{H8b-H9}$ = 5.5 Hz, 1H, H-8b), 1.64 (s, 9H, C(C*H*$_3$)$_3$–N*Boc* indole), 1.44 (s, 9H, C(C*H*$_3$)$_3$–*t*-butyl ester), 1.41 (s, 9H, C(C*H*$_3$)$_3$–NH*Boc*). $^{13}$C NMR ($CDCl_3$, 100 MHz) $\delta$: 170.9, 155.1, 149.5, 137.9, 134.2, 134.0, 131.0, 125.3, 124.2, 118.8, 115.5, 115.3, 115.0, 83.3, 82.1, 79.6, 54.2, 40.2, 28.3, 28.1, 27.9, 27.7. ESI-QTOF MS $m/z$ calculated for $C_{28}H_{40}N_2O_6$ $[M + H]^+$ 501.2959, measured 501.2975.

#### 4.2.12. Tert-butyl 3-(3-tert-butoxy-2-(tert-butoxycarbonylamino)-3-oxopropyl)-5-(3-hydroxypropyl)-1H-indole-1-carboxylate (**15**)

To a solution of **14** (200 mg, 0.4 mmol) in THF (2.7 ml) was added 9-BBN (0.5 M in THF, 1 ml, 0.52 mmol) and the clear colorless solution was stirred for 3 h at room temperature. The reaction mixture was then cooled at 0 °C and water (0.21 ml) was added slowly, followed by the addition of NaOH 3 M (0.21 ml, 0.62 mmol). Subsequently, $H_2O_2$ 30% (0.19 ml, 1.57 mmol) was added slowly within 5 min and then the reaction mixture was allowed to reach room temperature where it was stirred for 3 h. The organic layer was then separated from the biphasic system and the aqueous layer was extracted three times with ethyl acetate. The combined organic layers were washed once with water and brine, dried over sodium sulfate, filtered and evaporated to dryness. The crude was purified with flash column chromatography on silica gel using hexane/ethyl acetate 7:3 to yield the title compound as colorless oil (191 mg, 92%). $^1$H NMR ($CDCl_3$, 400 MHz) $\delta$ 8.03 (br, 1H, H-7), 7.38 (br, 2H, H-2 and H-4), 7.16 (dd, $^3J_{H6-H7}$ = 8.5 Hz, $^4J_{H6-H4}$ = 1.5 Hz, 1H, H-6), 5.16 (d, $J$ = 7.9 Hz, 1H, N*H*Boc), 4.60–4.48 (m, 1H, H-9), 3.66 (t, $J$ = 6.3 Hz, 2H, H-13), 3.23–3.08 (m, 2H, H-8), 2.81 (t, $J$ = 7.6 Hz, 2H, H-11), 2.01–1.83 (m, 2H, H-12), 1.64 (s, 9H, C(C*H*$_3$)$_3$–*N*-Boc indole), 1.43 (s, 9H, C(C*H*$_3$)$_3$–*t*-butyl ester), 1.40 (s, 9H, C(C*H*$_3$)$_3$–NH*Boc*). $^{13}$C NMR ($CDCl_3$, 100 MHz) $\delta$: 170.9, 155.1, 149.5, 136.0, 133.8, 130.9, 125.1, 124.1, 118.7, 115.3, 114.9, 83.3, 82.1, 79.7, 61.8, 54.1, 34.6, 31.9, 28.3, 28.1, 27.9. ESI-QTOF MS $m/z$ calculated for $C_{28}H_{42}N_2O_7$ $[M + H]^+$ 519.3065, measured 519.3058.

#### 4.2.13. Tert-butyl-3-(3-tert-butoxy-2-(tert-butoxycarbonylamino)-3-oxopropyl)-5-(3-(methylsul-fonyloxy)-propyl)-1H-indole-1-carboxylate (**16**)

A solution of mesyl chloride (123 mg, 1.08 mmol) in dichloromethane (0.6 ml) was added dropwise within 5 min to an ice cold solution of **15** (180 mg, 0.35 mmol) and triethylamine (0.15 ml, 1.08 mmol) in dichloromethane (1.2 ml) and reaction was stirred for 2 h at 0 °C. After this time, the reaction was diluted with DCM and washed once with saturated $NaHCO_3$ solution followed by water and brine, dried over sodium sulfate, filtered and concentrated to dryness under vacuum. The crude was purified with flash column chromatography using hexane/ethyl acetate 8:2 to yield the product as a clear colorless oil (197 mg, 95%). $^1$H NMR ($CDCl_3$, 400 MHz) $\delta$ 8.06 (br, 1H, H-7), 7.43–7.32 (m, 2H, H-2 and H-4), 7.15 (dd, $^3J_{H6-H7}$ = 8.5 Hz, $^4J_{H6-H4}$ = 1.6 Hz, 1H, H-6), 5.11 (d, $J$ = 7.9 Hz, 1H, N*H*Boc), 4.59–4.49 (m, 1H, H-9), 4.24 (t, $J$ = 6.4 Hz, 2H, H-13), 3.24–3.08 (m, 2H, H-8), 3.00 (s, 3H, C*H*$_3$S(=O)$_2$O–), 2.85 (t, $J$ = 7.4 Hz, 2H, H-11), 2.17–2.07 (m, 2H, H-12), 1.65 (s, 9H, C(C*H*$_3$)$_3$ NBoc-indole), 1.44 (s, 9H, C(C*H*$_3$)$_3$–*t*-butyl ester), 1.41 (s, 9H, C(C*H*$_3$)$_3$ NHBoc). $^{13}$C NMR ($CDCl_3$, 100 MHz) $\delta$: 170.9, 155.1, 149.5, 134.5, 134.1, 131.1, 125.0, 124.4, 118.7, 115.3, 115.2, 83.4, 82.1, 79.7, 69.1, 54.1, 37.3, 31.5, 31.2, 28.3, 28.1, 27.9. ESI-QTOF MS $m/z$ calculated for $C_{29}H_{44}N_2O_9S$ $[M + H]^+$ 597.2840, measured 597.2832.

#### 4.2.14. Tert-butyl-3-(3-tert-butoxy-2-(tert-butoxycarbonylamino)-3-oxopropyl)-5-(3-fluoropro-pyl)-1H-indole-1-carboxylate (**17**)

A suspension of mesylate **16** (197 mg, 0.33 mmol) and cesium fluoride (250 mg, 1.65 mmol) in *t*-BuOH (1.35 ml) was heated at 80 °C for 8 h. The reaction mixture was then diluted with ethyl acetate (30 ml), washed with water (2 × 15 ml) and brine (1 × 15 ml), the organic layer was dried over sodium sulfate and evaporated to dryness under reduced pressure. The crude was purified with flash column chromatography using hexane/ethyl acetate 9:1 to yield a white sticky solid (159 mg, 93%). $^1$H NMR ($CDCl_3$, 400 MHz) $\delta$ 8.05 (br, 1H, H-7), 7.39 (s, 1H, H-2), 7.35 (br, 1H, H-4), 7.16 (dd, $^3J_{H6-H7}$ = 7.3 Hz, $^4J_{H6-H4}$ = 1.6 Hz 1H, H-6), 5.11 (d, $J$ = 7.8 Hz, 1H, N*H*Boc), 4.60–4.51 (m, 1H, H-9), 4.46 (dt, $^2J_{H13-F}$ = 47.2 Hz, $^3J_{H13-H12}$ = 6.1 Hz, 2H, H-13), 3.25–3.07 (m, 2H, H-8), 2.84 (t, $J$ = 7.5 Hz, 2H, H-11), 2.13–1.97 (m, 2H, H-12), 1.64 (s, 9H, C(C*H*$_3$)$_3$ NBoc-indole), 1.43 (s, 9H, C(C*H*$_3$)$_3$ *t*-butyl ester), 1.41 (s, 9H, C(C*H*$_3$)$_3$ NH*Boc*). $^{13}$C NMR ($CDCl_3$, 100 MHz) $\delta$: 170.9, 155.1, 149.4, 135.3, 133.9, 131.0, 125.1, 124.3, 118.7, 115.2, 115.0, 83.3, 83.0 (d, $^1J_{C-F}$ = 165.1 Hz), 82.1, 79.6, 54.2, 32.6 (d, $^2J_{C-F}$ = 19.8 Hz), 31.3 (d, $^3J_{C-F}$ = 5.4 Hz), 28.3, 28.1, 27.9, 27.8. $^{19}$F NMR ($CDCl_3$, 376 MHz) $\delta$: −219.6 to −220.3. ESI-QTOF MS $m/z$ calculated for $C_{28}H_{41}FN_2O_6$ $[M + H]^+$ 521.3021, measured 521.3014.

#### 4.2.15. 2-Amino-3-(5-(3-fluoropropyl)-1H-indol-3-yl)propanoic acid (**18**)

TFA (0.67 ml, 8.74 mmol) was added dropwise to an ice cold mixture of compound **17** (35 mg, 0.067 mmol), dimethylsulfane (0.67 ml, 9.08 mmol) and ethane-1,2-dithiol (68 μl, 0.81 mmol) in dichloromethane (0.7 ml). The reaction was stirred for 10 min at 0 °C and then was allowed to reach room temperature where it was stirred for 3 h while being monitored with HPLC (5-FPTRP, $t_R$ = 13.2 min). After this time, the reaction was heated at 50 °C for 1 h and then the volatiles were removed under reduced pressure. The oil that remained was taken up in water (10 ml), washed with ether (3 × 5 ml) and then concentrated to an approximate volume of 3 ml. The mixture was purified with preparative HPLC. The product eluted approximately at 12.4 min and was obtained as a white solid after lyophilization (15.8 mg, 89%). $^1$H NMR ($d_6$-DMSO,

400 MHz) $\delta$ 10.98 (s, 1H, H-1), 8.46–8.17 (br, 3H, $-NH_3^+$), 7.40 (br, 1H, H-4), 7.30 (d, $^3J_{H7-H6}$ = 8.4 Hz, 1H, H-7), 7.19 (br d, $^3J_{H2-H1}$ = 2.3 Hz, 1H, H-2), 6.96 (dd, $^3J_{H6-H7}$ = 8.4 Hz, $^4J_{H6-H4}$ = 1.5 Hz, 1H, H-6), 4.46 (dm, $^2J_{H13-F}$ = 47.5 Hz, 2H, H-13), 4.14 (br, 1H, H-9), 3.27–3.21 (m, 2H, H-8), 2.78–2.70 (m, 2H, H-11), 2.06–1.92 (m, 2H, H-12). $^{13}$C NMR ($d_6$-DMSO, 100 MHz) $\delta$: 170.9 (C-10), 135.0 (C-7a), 131.0 (C-5), 127.3 (C-3a), 125.1 (C-2), 122.1 (C-6), 117.4 (C-4), 111.4 (C-7), 106.4 (C-3), 83.2 (d, $^1J_{C13-F}$ = 162 Hz, C-13), 52.7 (C-9), 32.5 (d, $^2J_{C12-F}$ = 18.8 Hz, C-12), 31.0 (d, $^3J_{C11-F}$ = 6.2 Hz, C-11), 26.2 (C-8). $^{19}$F NMR ($d_6$-DMSO, 376 MHz) $\delta$: −217.8 to −218.3 (m). ESI-QTOF MS *m/z* calculated for $C_{14}H_{17}FN_2O_2$ $[M + H]^+$ 265.1347, measured 265.1351.

### 4.3. Radiosynthesis of [$^{18}$F]2-FPTRP and [$^{18}$F]5-FPTRP

[$^{18}$F]-fluoride was obtained via the $^{18}$O(p,n)$^{18}$F reaction using 98% enriched $^{18}$O–water. $^{18}F^-$ was trapped on a light QMA cartridge (Waters), which was preconditioned with 0.5 M $K_2CO_3$ (5 mL) and water (5 mL). 0.7 mL of tetrabutylammonium bicarbonate ($TBAHCO_3$) solution (prepared from dissolving 933 mg TBAOH in 20 ml MeOH and bubbling with $CO_2$ to a pH ≈ 8) was used for the elution of $^{18}F^-$ from the cartridge. The solvent was evaporated at 110 °C under vacuum in the presence of slight inflow of nitrogen gas. After addition of acetonitrile (0.5 mL), azeotropic drying was carried out. This procedure was repeated twice to afford dry [$^{18}$F]TBAF. A solution of the corresponding fully *tert*-butyl protected mesylate precursor (5 mg in 0.6 ml dry acetonitrile) was added to the dried [$^{18}$F]TBAF. The reaction mixture was heated at 100 °C for 10 min and then evaporated to dryness under reduced pressure. To the crude was added 0.6 ml HCl 4 M solution and the reaction was heated at 100 °C for 10 min. The mixture was then neutralized by the addition of 0.57 ml NaOH 4 M solution and 1.4 ml of PBS 0.6 M containing 20 mg/ml sodium ascorbate (final pH ≈ 6). Purification was performed by semi-preparative HPLC, with [$^{18}$F]2-FPTRP eluting at about 21 min while [$^{18}$F]5-FPTRP at 26 min and they were collected in a vial containing 40 mg sodium ascorbate. The products were neutralized with sodium hydrogen carbonate (10%) to pH ≈ 6 and diluted with water for injection so as the final formulation would contain 20 mg/ml sodium ascorbate. The solutions were then passed through a sterile filter and used for *in vitro* and *in vivo* studies. Identification of [$^{18}$F]2-FPTRP or [$^{18}$F]5-FPTRP was confirmed by co-injection with references **10** and **18** respectively. Chemical and radiochemical purity were determined by analytical HPLC; $t_R$ = 10.9 min for [$^{18}$F]2-FPTRP and 11.4 min for [$^{18}$F]5-FPTRP. The radiochemical purity was always >99%. [$^{18}$F]FET was obtained from a routine clinical production from the University Hospital Zurich, Switzerland.

### 4.4. In vitro cell uptake and inhibition studies

NCI-H69 cells were purchased from CLS (Eppelheim, Germany) and were cultured according to the supplier's protocol. Experiments were conducted as described by us previously and under the same experimental conditions [24]. Cells were washed and pre-incubated for 1 h at 37 °C with Earle balanced salt solution containing $Ca^{2+}$ and $Mg^{2+}$ (EBSS, Invitrogen). The monoamine oxidase inhibitors clorgyline 0.1 mM (Sigma) and pargyline 0.1 mM (Acros Organics), and if indicated 10 mM of the LAT inhibitor BCH were added in EBSS together with the radiotracer (ca 20 kBq) at 37 or 4 °C and cells were incubated at the indicated temperature. The final tracer concentrations were in the range of 0.8–1 nM. Cells were washed twice with ice cold EBSS at the indicated time points. The radioactivity was quantified in a gamma counter (Wizard 1480, Perkin Elmer). To inhibit AADC, 80 μM *S*-carbidopa (Santa Cruz Biotechnology, Santa Cruz, CA, USA) was added in DMSO/100 mM PBS 30 min before tracer addition [24]. The final DMSO concentration was 0.3%. Cell viability was 80–90% after 60 min for all conditions as tested with trypan blue staining.

### 4.5. In vivo PET studies

*In vivo* experiments were approved by the Veterinary Office of the Canton Zurich and were conducted in accordance with the Swiss Animal Welfare legislation. Female NMRI nu/nu mice (Charles River, Sulzfeld, Germany) were inoculated at six weeks of age subcutaneously with $1 \times 10^7$ NCI-H69 cells in 100 μl PBS with $Ca^{2+}$ and $Mg^{2+}$ (Invitrogen; BP bioscience) on the right shoulder and 1 week $3 \times 10^6$later with the same cell number in matrigel (BD Biosciences) on the left shoulder. PC-3 xenografts were initiated with PC-3 cells (DSMZ, ACC-465) in 100 μl Matrigel on the right shoulder. PET/CT scans were performed two to five weeks after inoculation, when the tumor volumes reached 0.2–1.5 $cm^3$. Animals were injected into the tail vein with 10 MBq–14 MBq (0.17–0.27 nmol) of the corresponding amino acid radiotracer. For experiments with AADC inhibition, two NCI-H69 xenograft-bearing mice were injected intraperitoneally (i.p.) with either 25 mg/kg *S*-carbidopa or saline 60 min before tracer injection. Anesthesia with 2–3% isoflurane in oxygen/air was initiated 10 min before the PET scan and animals were monitored as described previously [24]. PET data was acquired with the small animal PET/CT camera VISTA eXplore (Sedecal, Spain; GE Healthcare) in list mode for dynamic analysis starting at 1, 30 (NCI-H69 xenografts only) or 60 min post p.i. and as static scans from 30 to 45 min p.i. for the comparison of tumor uptake with and without S-carbidopa. Data were reconstructed with the 2D ordered-subsets expectation maximization (2D-OSEM) protocol and analyzed with the software PMOD 3.3 (PMOD, Zurich, Switzerland). Regions of interest of the xenograft, a reference region on the contralateral shoulder or the neck region were drawn in PMOD according to the PET and CT images. Tissue radioactivity was expressed as SUV, i.e., the decay corrected radioactivity per $cm^3$ divided by the injected radioactivity dose per g body weight.

### 4.6. Ex vivo metabolite studies

[$^{18}$F]2-FPTRP or [$^{18}$F]5-FPTRP (80–120 or 60 MBq) was injected via a lateral tail vein into female 9–12 weeks old NMRI nu/nu mice bearing NCI-H69 xenografts. Blood samples were withdrawn via the opposite tail vein and animals were sacrificed by decapitation under isoflurane anesthesia at the indicated time points. Blood was collected and proteins were precipitated with an equal volume ice cold acetonitrile and centrifugation at 5000 × *g*, 4 °C for 5 min. Supernatants were filtered through 0.2 μm filters and analyzed by radio TLC. Normal phase TLC plates were used (aluminum sheets, silica gel 60 $F_{254}$, Merck). The mobile phase was DCM/MeOH/$NH_4OH$ (25%) 70:30:2.5. Developed TLCs were visualized with InstantImager (Canberra Packard). Conditions for UPLC analysis are the same with the ones used for radiosynthesis control.

### 4.7. Statistical analysis

Cell uptake and PET SUV ratios between xenografts and reference tissue were analyzed by two-tailed homoscedastic Student's *t*-test. $P < 0.05$ were considered significant. Average values are shown with standard deviations.

## References

[1] C. Plathow, W.A. Weber, Tumor cell metabolism imaging, J. Nucl. Med. 49 (2008) 43s–63s.

[2] O. Couturier, J.F. Chatal, R. Hustinx, Fluorinated analogs of nucleosides and fluorinated tracers of gene expression for positron emission tomography, Bull. Cancer 91 (2004) 695–703.
[3] P.S. Conti, D.L. Lilien, K. Hawley, J. Keppler, S.T. Grafton, J.R. Bading, PET and [F-18]-FDG in oncology: a clinical update, Nucl. Med. Biol. 23 (1996) 717–735.
[4] G.J. Kelloff, K.A. Krohn, S.M. Larson, R. Weissleder, D.A. Mankoff, J.M. Hoffman, J.M. Link, K.Z. Guyton, W.C. Eckelman, H.I. Scher, J. O'Shaughnessy, B.D. Cheson, C.C. Sigman, J.L. Tatum, G.Q. Mills, D.C. Sullivan, J. Woodcock, The progress and promise of molecular imaging probes in oncologic drug development, Clin. Cancer Res. 11 (2005) 7967–7985.
[5] J. Barentsz, S. Takahashi, W. Oyen, R. Mus, P. De Mulder, R. Reznek, M. Oudkerk, W. Mali, Commonly used imaging techniques for diagnosis and staging, J. Clin. Oncol. 24 (2006) 3234–3244.
[6] E.K.J. Pauwels, M.J. Ribeiro, J.H.M.B. Stoot, V.R. McCready, M. Bourguignon, B. Maziere, FDG accumulation and tumor biology, Nucl. Med. Biol. 25 (1998) 317–322.
[7] J. McConathy, W.P. Yu, N. Jarkas, W. Seo, D.M. Schuster, M.M. Goodman, Radiohalogenated nonnatural amino acids as PET and SPECT tumor imaging agents, Med. Res. Rev. 32 (2012) 868–905.
[8] P. Laverman, O.C. Boerman, F.H.M. Corstens, W.J.G. Oyen, Fluorinated amino acids for tumour imaging with positron emission tomography, Eur. J. Nucl. Med. Mol. Imaging 29 (2002) 681–690.
[9] J. McConathy, M.M. Goodman, Non-natural amino acids for tumor imaging using positron emission tomography and single photon emission computed tomography, Cancer Metastasis Rev. 27 (2008) 555–573.
[10] B.C. Fuchs, B.P. Bode, Amino acid transporters ASCT2 and LAT1 in cancer: partners in crime? Semin. Cancer Biol. 15 (2005) 254–266.
[11] H. Nawashiro, N. Otani, N. Shinomiya, S. Fukui, H. Ooigawa, K. Shima, H. Matsuo, Y. Kanai, H. Endou, L-type amino acid transporter 1 as a potential molecular target in human astrocytic tumors, Int. J. Cancer 119 (2006) 484–492.
[12] O. Yanagida, Y. Kanai, A. Chairoungdua, D.K. Kim, H. Segawa, T. Nii, S.H. Cha, H. Matsuo, J. Fukushima, Y. Fukasawa, Y. Tani, Y. Taketani, H. Uchino, J.Y. Kim, J. Inatomi, I. Okayasu, K. Miyamoto, E. Takeda, T. Goya, H. Endou, Human L-type amino acid transporter 1 (LAT1): characterization of function and expression in tumor cell lines, BBA Biomembr. 1514 (2001) 291–302.
[13] K.J. Langen, K. Hamacher, M. Weckesser, F. Floeth, G. Stoffels, D. Bauer, H.H. Coenen, D. Pauleit, *O*-(2-[(18)F]Fluoroethyl)-L-tyrosine: uptake mechanisms and clinical applications, Nucl. Med. Biol. 33 (2006) 287–294.
[14] H.J. Wester, M. Herz, W. Weber, P. Heiss, R. Senekowitsch-Schmidtke, M. Schwaiger, G. Stocklin, Synthesis and radiopharmacology of O-(2-[F-18] fluoroethyl)-L-tyrosine for tumor imaging, J. Nucl. Med. 40 (1999) 205–212.
[15] K.J. Langen, D. Pauleit, H.H. Coenen, 3-[I-123]iodo-alpha-methyl-L-tyrosine: uptake mechanisms and clinical applications, Nucl. Med. Biol. 29 (2002) 625–631.
[16] A. Lilja, K. Bergstrom, P. Hartvig, B. Spannare, C. Halldin, H. Lundqvist, B. Langstrom, Dynamic study of supratentorial gliomas with L-methyl-C-11-methionine and positron emission tomography, Am. J. Neuroradiol. 6 (1985) 505–514.
[17] T.M. Shoup, J. Olson, J.M. Hoffman, J. Votaw, D. Eshima, L. Eshima, V.M. Camp, M. Stabin, D. Votaw, M.M. Goodman, Synthesis and evaluation of [(18)F]1-amino-3-fluorocyclobutane-1-carboxylic acid to image brain tumors, J. Nucl. Med. 40 (1999) 331–338.
[18] O.C. Neels, K.P. Koopmans, P.L. Jager, L. Vercauteren, A. van Waarde, J. Doorduin, H. Timmer-Bosscha, A.H. Brouwers, E.G.E. de Vries, R.A.J.O. Dierckx, I.P. Kema, P.H. Elsinga, Manipulation of [C-11]-5-hydroxytryptophan and 6-[F-18]fluoro-3,4-dihydroxy-L-phenylalanine accumulation in neuroendocrine tumor cells, Cancer Res. 68 (2008) 7183–7190.
[19] J. Vachtenheim, H. Novotna, Expression of the aromatic L-amino acid decarboxylase mRNA in human tumour cell lines of neuroendocrine and neuroectodermal origin, Eur. J. Cancer 33 (1997) 2411–2417.
[20] K.P. Koopmans, O.N. Neels, I.P. Kema, P.H. Elsinga, T.P. Links, E.G.E. de Vries, P.L. Jager, Molecular imaging in neuroendocrine tumors: molecular uptake mechanisms and clinical results, Crit. Rev. Oncol. Hemat. 71 (2009) 199–213.
[21] A. Sundin, B. Eriksson, M. Bergstrom, B. Langstrom, K. Oberg, H. Orlefors, PET in the diagnosis of neuroendocrine tumors, Ann. N Y Acad. Sci. 1014 (2004) 246–257.
[22] A.G.E. Pearse, APUD – concept, tumors, molecular markers and amyloid, Mikroskopie 36 (1980) 257–269.
[23] P. Bjurling, Y. Watanabe, M. Tokushige, T. Oda, B. Langstrom, Syntheses of beta-C-11-labeled L-tryptophan and 5-hydroxy-L-tryptophan using a multienzymatic reaction route, J. Chem. Soc. Perkin Trans 1 (1989) 1331–1334.
[24] S.D. Krämer, L.J. Mu, A. Muller, C. Keller, O.F. Kuznetsova, C. Schweinsberg, D. Franck, C. Muller, T.L. Ross, R. Schibli, S.M. Ametamey, 5-(2-F-18-Fluoroethoxy)-L-tryptophan as a substrate of system L transport for tumor imaging by PET, J. Nucl. Med. 53 (2012) 434–442.
[25] R.F. Li, S.C. Wu, S.C. Wang, Z. Fu, Y.H. Dang, L. Huo, Synthesis and evaluation of L-5-(2-[F-18]fluoroethoxy)tryptophan as a new PET tracer, Appl. Radiat. Isot. 68 (2010) 303–308.
[26] T. Sun, G.H. Tang, H. Tian, X.Y. Wang, X.H. Chen, Z.F. Chen, S.C. Wang, Radiosynthesis of 1-[F-18]fluoroethyl-L-tryptophan as a novel potential amino acid PET tracer, Appl. Radiat. Isotopes 70 (2012) 676–680.
[27] W. Lovenberg, H. Weissbach, S. Udenfriend, Aromatic L-amino acid decarboxylase, J. Biol. Chem. 237 (1962) 89–93.
[28] D.N. Carney, A.F. Gazdar, G. Bepler, J.G. Guccion, P.J. Marangos, T.W. Moody, M.H. Zweig, J.D. Minna, Establishment and identification of small cell lung-cancer cell-lines having classic and variant features, Cancer Res. 45 (1985) 2913–2923.
[29] M. Avgeris, G. Koutalellis, E.G. Fragoulis, A. Scorilas, Expression analysis and clinical utility of L-dopa decarboxylase (DDC) in prostate cancer, Clin. Biochem. 41 (2008) 1140–1149.
[30] S. Oka, H. Okudaira, Y. Yoshida, D.M. Schuster, M.M. Goodman, Y. Shirakami, Transport mechanisms of trans-1-amino-3-fluoro[1-C-14] cyclobutanecarboxylic acid in prostate cancer cells, Nucl. Med. Biol. 39 (2012) 109–119.
[31] E. Miko, Z. Margitai, Z. Czimmerer, I. Varkonyi, D. Balazs, A. Lanyi, Z. Bacso, B. Scholtz, miR-126 inhibits proliferation of small cell lung cancer cells by targeting SLC7A5, FEBS Lett. 585 (2011) 1191–1196.
[32] J.M. Schkeryantz, J.C.G. Woo, P. Siliphaivanh, K.M. Depew, S.J. Danishefsky, Total synthesis of gypsetin, deoxybrevianamide E, brevianamide E, and tryprostatin B: novel constructions of 2,3-disubstituted indoles, J. Am. Chem. Soc. 121 (1999) 11964–11975.
[33] T. Nagasaka, S. Ohki, Indoles .2. Oxidation of *N*-phthaloyl-1-acetyltryptophan with chromium trioxide, Chem. Pharm. Bull 19 (1971) 603–611.
[34] Y.Q. Feng, G. Chen, Total synthesis of celogentin C by stereoselective C–H activation, Angew. Chem. Int. Ed. 49 (2010) 958–961.
[35] A.L. Smith, C.K. Hwang, E. Pitsinos, G.R. Scarlato, K.C. Nicolaou, Enantioselective total synthesis of (–)-calicheamicinone, J. Am. Chem. Soc. 114 (1992) 3134–3136.
[36] A. Furst, R.C. Berlo, S. Hooton, Hydrazine as a reducing agent for organic compounds (Catalytic hydrazine reductions), Chem. Rev. 65 (1965) 51–68.
[37] V.P. Agrawal, Hydrazinolysis of lipids and analysis of their constituent fatty-acids, J. Lipid Res. 24 (1983) 216–220.
[38] D.W. Kim, H.J. Jeong, S.T. Litn, M.H. Sohn, J.A. Katzenellenbogen, D.Y. Chi, Facile nucleophilic fluorination reactions using *tert*-alcohols as a reaction medium: significantly enhanced reactivity of alkali metal fluorides and improved selectivity, J. Org. Chem. 73 (2008) 957–962.
[39] B.F. Lundt, N.L. Johansen, A. Volund, J. Markussen, Removal of *tert*-butyl and *tert*-butoxycarbonyl protecting groups with trifluoroacetic-acid – mechanisms, bi-product formation and evaluation of scavengers, Int. J. Pept. Prot. Res. 12 (1978) 258–268.
[40] M. Bodanszky, A. Bodanszky, Improved selectivity in the removal of the *tert*-butyloxycarbonyl group, Int. J. Pept. Prot. Res. 23 (1984) 565–572.
[41] Y. Masui, N. Chino, S. Sakakibara, Modification of tryptophyl Residues during the acidolytic cleavage of Boc-groups .1. Studies with Boc-tryptophan, Bull. Chem. Soc. Jpn. 53 (1980) 464–468.
[42] P.Z. Decroos, P. Sangdee, B.L. Stockwell, L. Kar, E.B. Thompson, M.E. Johnson, B.L. Currie, Hemoglobin-S antigelation agents based on 5-bromotryptophan with potential for sickle-cell-anemia, J. Med. Chem. 33 (1990) 3138–3142.
[43] S. Kotha, M. Behera, V.R. Shah, A simple synthetic approach to allylated aromatics via the Suzuki–Miyaura cross-coupling reaction, Synlett (2005) 1877–1880.
[44] E.R. Stadtman, Oxidation of free amino-acids and amino-acid-residues in proteins by radiolysis and by metal-catalyzed reactions, Annu. Rev. Biochem. 62 (1993) 797–821.
[45] L.M. Wang, B.P. Lieberman, K. Plossl, W.C. Qu, H.F. Kung, Synthesis and comparative biological evaluation of L- and D-isomers of F-18-labeled fluoroalkyl phenylalanine derivatives as tumor imaging agents, Nucl. Med. Biol. 38 (2011) 301–312.
[46] P. Heiss, A. Mayer, M. Herz, H.J. Wester, M. Schwaiger, R. Senekowitsch-Schmidtke, Investigation of transport mechanism and uptake kinetics of *O*-(2-[F-18]fluoroethyl)-L-tyrosine in vitro and in vivo, J. Nucl. Med. 40 (1999) 1367–1373.
[47] K.J. Langen, K. Hamacher, D. Bauer, S. Broer, D. Pauleit, H. Herzog, F. Floeth, K. Zilles, H.H. Coenen, Preferred stereoselective transport of the D-isomer of cis-4-[F-18]fluoro-proline at the blood–brain barrier, J. Cereb. Blood Flow Metab. 25 (2005) 607–616.
[48] H. Tsukada, K. Sato, D. Fukumoto, T. Kakiuchi, Evaluation of D-isomers of O-F-18-fluoromethyl, O-F-18-fluoroethyl and O-F-18-fluoropropyl tyrosine as tumour imaging agents in mice, Eur. J. Nucl. Med. Mol. Imaging 33 (2006) 1017–1024.
[49] M.J. Mintz, C. Walling, *t*-Butyl hypochlorite, Org. Synth. Coll. Vol. 5 (1973) 184, 49 (1969), p. 9, http://www.orgsyn.org/orgsyn/orgsyn/prepContent.asp?prep=cv5p0184.